Observations of the 40–50-Day Tropical Oscillation—A Review

ROLAND A. MADDEN

National Center for Atmospheric Research, Boulder, Colorado*

PAUL R. JULIAN

National Meteorological Center, Washington, D.C.

(Manuscript received 4 January 1993, in final form 25 August 1993)

ABSTRACT

Observational aspects of the 40–50-day oscillation are reviewed. The oscillation is the result of large-scale circulation cells oriented in the equatorial plane that move eastward from at least the Indian Ocean to the central Pacific. Anomalies in zonal winds and the velocity potential in the upper troposphere often propagate the full circumference of the globe. Related, complex convective regions also show an eastward movement. There is a zonally symmetric component to the oscillation. It is manifest in changes in surface pressure and in the relative atmospheric angular momentum. The oscillation is an important factor in the timing of active and break phases of the Indian and Australian monsoons. It affects ocean waves, currents, and air–sea interaction. The oscillation was particularly active during the First GARP (Global Atmospheric Research Program) Global Experiment year, and some features that were evident during the Monsoon Experiment are described.

1. Introduction

Reviewing the literature on the phenomenon that we (Madden and Julian 1971) called the 40–50-day oscillation (hereafter referred to as the oscillation) is not an easy task. It is not possible for us to identify for certain which of the many aspects of the oscillation that have been reported will prove to be most important. There has been considerable literature on the subject in the period since 1979. It was then that Yasunari's work (Yasunari 1979) related the eastward-propagating, near-equatorial oscillation that we had described to active and break periods of the Indian summer monsoon. The First GARP (Global Atmospheric Research Program) Global Experiment (FGGE) also took place during that year and provided the most complete global dataset available to that time. Lorenc (1984) used the dataset to show a regular eastward propagation of the upper-tropospheric velocity potential χ and its close relation to the active and break monsoon periods. Many other authors studied these data and revealed previously unknown features of the oscillation. Here, we describe what we judge to be some of the most important findings from studies of these and of other data.

The discussion concentrates on eastward-moving cloud complexes that are associated with the oscillation, the northward-propagating cloud zones related to the break and active phases during the northern summer monsoon, some possible effects in the extratropics, atmospheric angular momentum changes, and effects in the ocean. Active workers in the field will find nothing new in this review. We hope that it will bring those who want a general knowledge of the oscillation up to date. The review deals only with observational studies. We have, for the most part, neglected a considerable body of theoretical and modeling work aimed at explaining the oscillation.

2. Background

In the late 1960s tropical data were sparse, as they still are in many areas. Spectral analysis was beginning to be used effectively to extract information from rawinsonde data collected at widely scattered observing stations. Maruyama (1967, 1968) had used it to describe the mixed Rossby–gravity waves in the equatorial stratosphere that Yanai and he had discovered (Yanai and Maruyama 1966). Wallace and Kousky (1968) used it to identify stratospheric Kelvin waves. These papers influenced us along with ones by Yanai et al. (1968) and Wallace and Chang (1969). In them, the authors again used spectrum analysis to describe—

* The National Center for Atmospheric Research is sponsored by the National Science Foundation.

Corresponding author address: Dr. Roland A. Madden, NCAR/Climate Analysis Section, P.O. Box 3000, Boulder, CO 80307-3000.

this time—tropospheric, synoptic-scale features in the tropics.

In those days, long time series were not readily available from tropical rawinsonde stations, nor were they easy to process with the computers of the time. The above authors were constrained to use time series that ranged from only three months to two years long. We thought that we could add to their findings because the National Center for Atmospheric Research's (NCAR) Data Support Section had begun to collect rawinsonde data from around the world and had data from at least one tropical station, Canton Island[1] (2.8°S, 171.7°W), for nearly a ten-year period. We also had access at NCAR to the biggest computer available to atmospheric scientists (Control Data Corporation 6600).

After computing spectra and cross spectra of variables from the Canton rawinsondes, we noticed large coherence between surface pressure, zonal winds, and temperatures at various levels over a broad period range that maximized between 41 and 53 days (Madden and Julian 1971). The spectra of these variables also had relative maxima, or peaks, at these periods. The coherences exceeded zero and the spectral peaks exceeded a smooth background continuum at levels passing stringent a posteriori tests for statistical significance. The a posteriori tests were required because we had no beforehand theoretical evidence that extra variance or coherence should occur in this period range. Surface pressure was coherent and in phase with the 850-hPa zonal (u) wind, and coherent and nearly out of phase (within a tenth of a cycle) with temperatures from 700 to 150 hPa. The 850-hPa u was coherent and out of phase with the u wind from 300 to 100 hPa. We found little evidence that the meridional (v) wind played a role in the variations. These results are consistent with an oscillation that is—at 850 hPa at least—in approximate geostrophic balance with varying pressure maxima and minima centered on the equator. A low-level low pressure anomaly at the equator is accompanied by low-level anomalous easterly winds at Canton.

Spectra and cross spectra with data from other stations revealed spectral peaks and also marked maxima in coherence in the 40–50-day range between stations far removed from one another (Madden and Julian 1972a). Figure 1 is an example of coherence between surface pressure at Canton Island and Balboa in Panama (9.0°N, 79.6°W). There are two frequency bands that are highly coherent. One is at 5–6-day periods and the other extends from 12- to 100-day periods with the maximum at 40–50 days. There is an interesting difference between the phase angles in these two period ranges. At 5–6 days Balboa leads Canton (westward propagation), and at the longer periods Canton leads

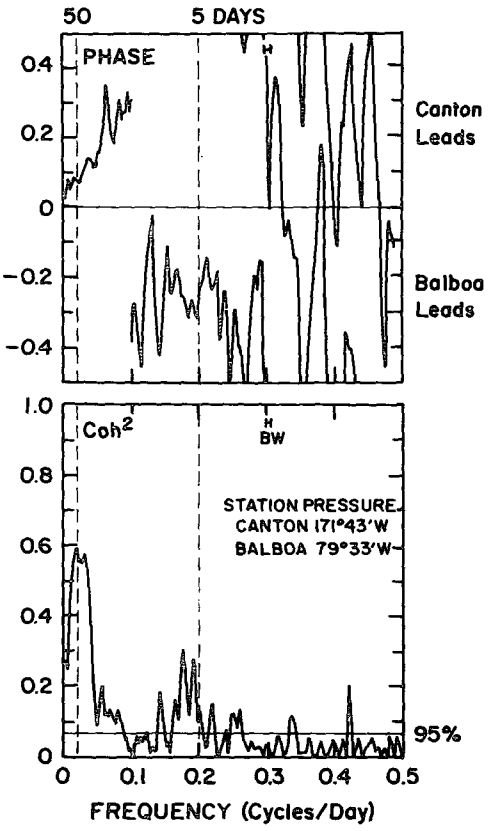

FIG. 1. Coherence squared (bottom) and phase in fractions of a cycle between the surface pressures at Canton (2.8°S, 171.7°W) and Balboa (9.0°N, 79.6°W) for the period 16 December 1959–24 March 1967. The bandwidth and the 95% limit for a null hypothesis of zero coherence are indicated.

Balboa (eastward propagation). The longitudinal separation between these two stations is 92° and the phase at 5–6-day periods is about 90° (0.2–0.3 cycles), consistent with a propagating disturbance of zonal wavenumber 1 scale. This westward-propagating disturbance appears to be the global scale, 5-day Rossby wave (Madden and Julian 1972b).

The nearly linear increase in phase with increasing frequency for the longer-period variations is consistent with disturbances that reach Balboa three days after they affect Canton. That is a longitudinal propagation speed of 39 m s^{-1}. There were peaks and coherence in surface pressure cross spectra between stations from the east coast of Africa to the western half of South America. Phase angles indicated a 20 m s^{-1} eastward propagation from Gan Island (0.7°S, 73.2°E) in the Indian Ocean to Canton Island in the Pacific (Fig. 2). Evidence of such rapid propagation suggested that the disturbance must in addition have characteristics of a standing oscillation in order that it may be reflected in a period on the order of 45 days in a single station time series.

[1] Now Kanton.

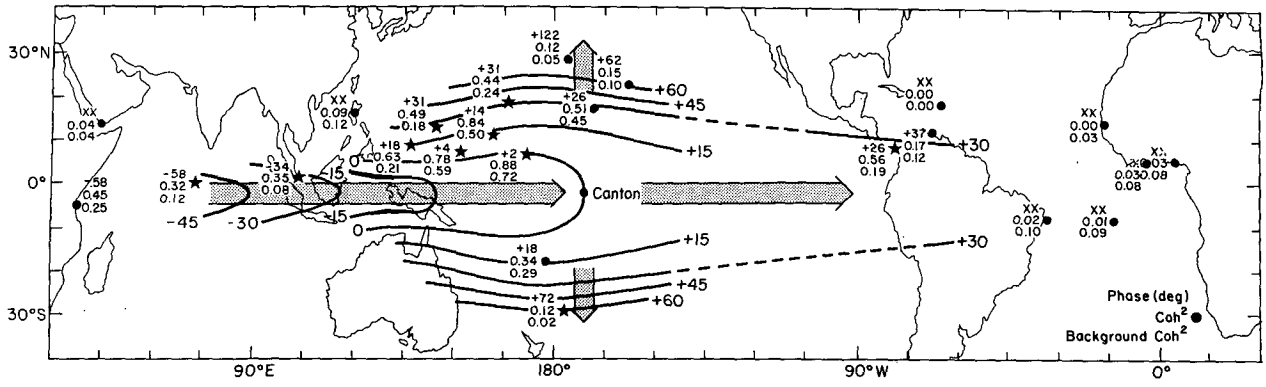

FIG. 2. Mean phase angles (deg), coherence squares, and background coherence squares for approximately the 36–50-day period range of cross spectra between surface pressures at all stations and those at Canton. The plotting model is given in the lower right-hand corner. Positive phase angle means Canton time series leads. Stars indicate stations where coherence squares exceed a smooth background at the 95% level. Mean coherence squares at Shemya (52.8°N, 174.1°E) and Campbell Island (52.6°S, 169.2°E) (not shown) are 0.08 and 0.02, respectively. Both are below their average background coherence squares. Values at Dar es Salaam (0.8°S, 39.3°E) are from a cross spectrum with Nauru. The arrows indicate propagation direction (adapted from Madden and Julian 1972).

There was a slower poleward propagation of about 2 m s^{-1} over the Pacific that we did not study. We had no data over Asia so we were unaware of a northward propagation of 1–2 m s^{-1} that is very important for the Indian summer monsoon. This feature is discussed in section 6. The 40–50-day surface pressure spectral peaks were approximately confined to ±10° of the equator, but relative maxima in coherence extended north from Canton to Midway (28.2°N, 177.4°W) and south to Raoul Island (29.2°S, 177.9°W).

Lower-tropospheric *u* winds from Singapore (1.4°N, 103.9°E) to Canton exhibited spectral peaks and coherence with the Canton pressure in the 40–50-day range. Variations in upper-tropospheric *u* winds from near-equatorial stations resulted in spectral peaks and in peaks in their coherence with Canton pressure the full circumference of the globe. Phases with Canton pressure indicated an eastward propagation at a rate slower than that of the pressure.

The sum of the evidence suggested that the oscillations were the result of an eastward movement of large-scale circulation cells oriented in the equatorial plane as depicted schematically in Fig. 3. Because we found no evidence of the oscillation in the lower troposphere over the Atlantic or western Africa, we assumed that it originated somewhere in the Indian Ocean. The indicated convection was supported by the convergence (divergence) in the lower-(upper) level *u* winds and by mixing ratios and temperatures.

From Fig. 3 it is clear that the near-geostrophic balance with equatorial-centered pressure oscillations that was suggested at 850 hPa at Canton (Madden and Julian 1971) is not found at all longitudes. Even at Truk[2] (7.4°N, 151.8°E) only 4000 km to the west the *u* wind at 850 hPa led the surface pressure perturbation by about 0.25 cycles (Madden and Julian 1972a, Fig. 8). Recently, Nishi (1989) quantified the relation between geopotential height *z* and the *u* wind with cross-spectral analyses. He found that in the lower troposphere 30–60-day variations in *z* and *u* are in phase only near the date line, while *u* tends to lead *z* by 0.33 cycles over India and Indonesia. We made similar calculations of phase angles between *z* and *u* at 45-day periods to present in Table 1. The lower-tropospheric in-phase relation is seen only near the date line at Canton and Majuro (7.1°N, 171.4°E), as pointed out by Nishi. Evidence for an in-phase relation is also present in the upper troposphere at Gan. For geostrophic balance the in-phase relationship is consistent with maximum pressure variations at the equator, while the more nearly out-of-phase relationship suggests maximum pressure variations off the equator.

The fact that the pressure anomalies do not add to zero along the equator (see times A and E in Fig. 3) indicates that mass flows in and out of the equatorial belt with the oscillation. Later we will see that a mean zonal or wavenumber zero component is manifest in an oscillation in the atmospheric angular momentum.

We pointed out that the oscillation was a broadband one and that spectra from different periods differed in detail. For example, Canton surface pressure data from 1 June 1957 to 27 April 1962 had a peak at 46 days, while that from 28 April 1962 to 24 March 1967 had a peak at 33 days. For pressure data at Balboa from roughly the same periods the spectral peaks were at 48 and 33 days (Madden and Julian 1972a). Figure 4 illustrates a similar difference in the spectra of Truk Island pressure data for two additional periods. Nevertheless, the overall character and the presence of the

[2] Now Chuuk.

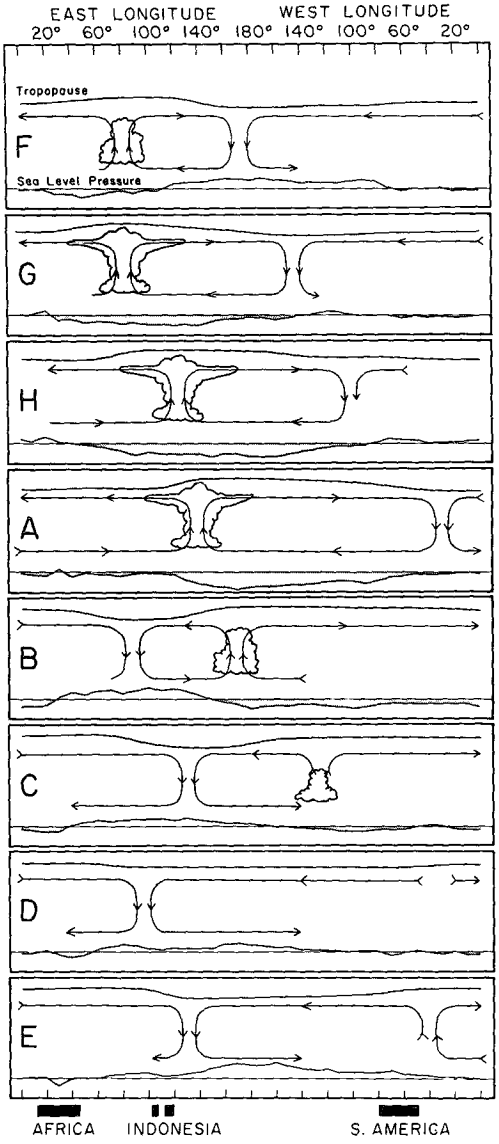

FIG. 3. Schematic depiction of the time and space (zonal plane) variations of the disturbance associated with the 40–50-day oscillation. Dates are indicated symbolically by the letters at the left of each chart and correspond to dates associated with the oscillation in Canton's station pressure. The letter A refers to the time of low pressure at Canton and E is the time of high pressure there. The other letters represent intermediate times. The mean pressure disturbance is plotted at the bottom of each chart with negative anomalies shaded. The circulation cells are based on the mean zonal wind disturbance. Regions of enhanced large-scale convection are indicated schematically by the cumulus and cumulonimbus clouds. The relative tropopause height is indicated at the top of each chart (taken from Madden and Julian 1972a).

oscillation has some stationarity in time. This was demonstrated by cross spectra of data recorded during the 1890s at Nauru Island (0.4°S, 161.0°E) and at Dar es Salaam (0.8°S, 39.3°E). Figure 5 is the spectrum of pressure at Nauru. It is very similar to that for Canton Island pressure observed from 1957 to 1967 and to that for Truk pressure from 1967 to 1979. We also found the coherence and phase based on these older data (shown in Fig. 2) to be consistent with eastward propagation.

3. Observations during the 1970s

In 1973 Parker reported results of a study of upper-tropospheric and lower-stratospheric equatorial winds (Parker 1973). He found the oscillation in the 100-hPa u winds and temperatures. Parker looked at several years of data during the 1960s but concentrated on the January–May 1966 period when the oscillation was particularly marked. He found it at equatorial stations all the way around the earth. The v wind did not appear to play a role. In the eastern hemisphere the 100-hPa temperature tended to lead the 100-hPa u wind by 0.25 cycles [parallel result for Truk and Canton in Madden and Julian (1972a, Fig. 8)], and over Gan Island at least, the 100-hPa height and u wind were in phase (seen also at 150 hPa in Table 1), indicating a geostrophic balance if the maximum pressure variations were at the equator. The oscillation also fell off in amplitude away from the equator. Its progression was irregular though, moving relatively fast from 140°W to the Greenwich meridian, moving more slowly near the date line. The average speed was near 13 m s^{-1}. These findings were in reasonably good agreement with ours for the very high troposphere. Parker considered the oscillation to be sufficiently like a Kelvin wave to be considered as such.

Dakshinamurti and Keshavamurty (1976) computed spectral analyses of the 850-hPa u and v winds over India and found 30-day peaks. Dakshinamurti and Keshavamurty suggested that these variations were associated with north–south oscillations of the monsoon trough. This is the northward propagation of the trough that has been studied extensively in recent years and is discussed here in section 6. To our knowledge there were no other published analyses of local winds that related to the oscillation during the decade.

The first published evidence based on actual cloud data that there might be eastward-propagating cloud systems similar to those of Fig. 3 came from Gruber (1974). He computed space–time spectra of satellite cloud brightness data from May through October of 1967. He found relative maxima for eastward propagation at a period of 50 days, for zonal wave 1 at the equator, 5°N, and 10°N. The 50-day eastward maximum was not evident in data from 15°N. Zangvil (1975) showed the eastward-moving clouds with a time–longitude diagram at the equator. His analysis of the wavelength, however, suggested that it was closer to wave 2 than wave 1. Zangvil also presented space–time spectra that had evidence of wave 1 and 2, 40-

day, eastward variance. During northern summer (1967) the maximum activity was along 5° and 10°N, and during northern winter (1967/68) it was at the equator and 5°S. This is consistent with maximum 40–50-day cloud activity residing in the vicinity of the intertropical convergence zone (ITCZ).

We consider 1979 to be a breaking point in the study of the oscillation and that is why we have treated observations during the 1970s as a separate section. In what follows we summarize some of the features of the oscillation that have been described primarily during the 1980s and early 1990s. The summary is broken up into sections on the time scale of the oscillation, related cloud anomalies, the role of the oscillation in the Indian and Australian monsoons, effects in the extratropics, anomalies in the atmospheric angular momentum, seasonal variations, anomalies in the oceans, and finally a survey of the literature dealing with the oscillation during the Monsoon Experiment (MONEX) of FGGE.

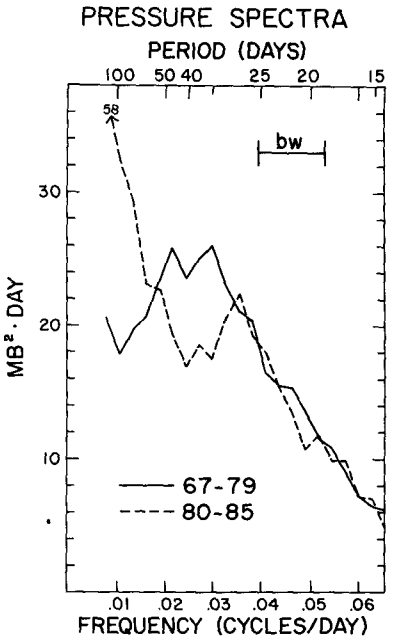

FIG. 4. Spectra of Truk (7.4°N, 151.8°E) pressure for two periods (1967–79 and 1980–85). Ordinate is variance per unit frequency. The bandwidth (bw) is indicated. The spectral estimate at 3/365 day^{-1} for the 1980–85 data is off the scale and equal to 58 mb^2 day (taken from Madden 1987).

4. On the time scale of the oscillation

In our first paper, we referred to the oscillation as the "40–50-day oscillation" (Madden and Julian 1971). It was in this range (actually 41–53 days) that spectra and cross spectra of the 10-yr record of upper-air data from Canton Island showed peaks or relative maxima. In the case of the coherence between variables there were more often than not absolute maxima in this period range. We did acknowledge that the oscillation was a relatively broadband phenomenon and not a highly tuned periodicity. After examining data from more stations and for different time periods we pointed out that the 40–50-day bounds were only approximate ones for the period of the responsible physical phenomenon (Madden and Julian 1972a). To further emphasize the broadband nature of the oscillation it is often referred to as the 30–50- and the 30–60-day oscillation (Krishnamurti and Subrahmanyam 1982; Weickmann et al. 1985; and many others). The broadband nature of the oscillation is evident in Figs. 1 and 5, and the changing frequency of the associated peak in the spectra is demonstrated in Fig. 4. The shift of the spectral

TABLE 1. Phase in fractions of a cycle between z and u at a 45-day period (0.02214 day^{-1}). Results are based on 2304-day time series beginning on the first of the indicated month. Associated coherence squares have approximately 46 degrees of freedom, so the 95% limit for a null hypothesis of zero coherence is 0.13. Only phase angles whose coherence square exceeds 0.13 are given. Entries of M denote levels where no cross spectra were computed. Positive phase angles mean u leads z.

				Level (hPa)									
Station	Latitude	Longitude	Start	1000	850	700	500	400	300	200	150	100	80
Canton	3°S	172°W	7/54	0.06	0.09		0.46					0.33	
Majuro	7°N	171°E	7/61		0.06		−0.49	0.44	0.34	0.28	0.26		
Truk	7°N	152°E	7/65				0.47						
Koror	7°N	134°E	7/61	0.34	0.35	0.36							
Singapore	1°N	104°E	1/65	M	0.20	−0.48				−0.47	−0.48	M	M
Cocos	12°S	97°E	7/57	0.37	0.33				−0.28				
Gan	1°S	73°E	1/65		0.34	0.32			−0.27		−0.06	M	M
Nairobi	1°S	37°E	7/59	M	M					M	M	M	M
Ascension	8°S	14°W	7/59										
Dakar	15°N	18°W	7/55			0.48	0.45		M	0.44	M	M	M
Piarco	11°N	61°W	7/72						0.26	0.23	0.17	0.23	0.31
Lima	12°S	77°W	7/58									M	M
Balboa	9°N	80°W	7/52	M			0.41						

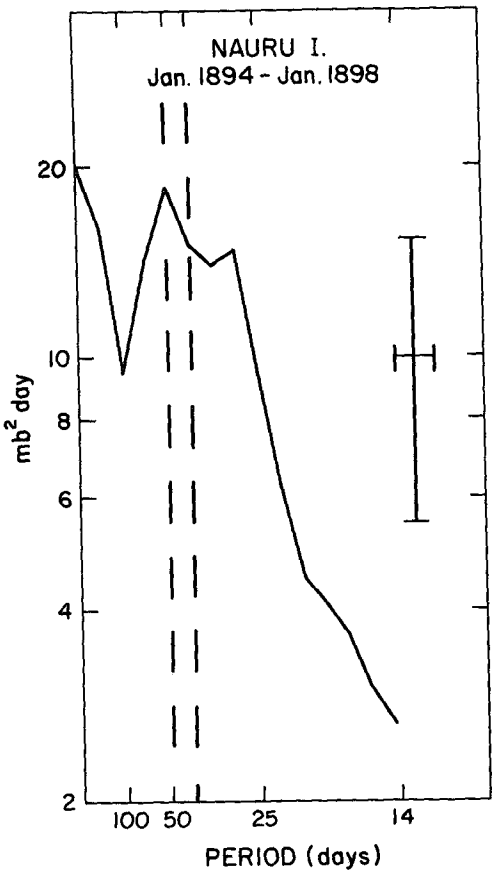

FIG. 5. Variance spectrum for station pressures at Nauru Island, 0.4°S, 161.0°E. Ordinate (variance/frequency) is logarithmic and abscissa (frequency) is linear. The 40–50-day period range is indicated by the dashed vertical lines. Prior 95% confidence limits and the bandwidth of the analysis (0.008 day^{-1}) are indicated by the cross (taken from Madden and Julian 1972).

peak to a 26-day period during the 1980–85 period and the strong 1982/83 warm event are consistent with suggestions that the oscillation tends to have a higher frequency during warm water or El Niño–Southern Oscillation (ENSO) years (Gray 1988; Kuhnel 1989).

The oscillation manifests itself in many variables. To study the period, we choose the u winds at Truk Island to serve as an index. In Fig. 6 are histograms of the periods of observed oscillations in Truk's u wind at 150 hPa. These periods were estimated subjectively by examining the time series of the wind. The average period is 45 days (48 days for September, October, and November) with a wide spread from the 22 to 79 days. There is no obvious change in the average period with season. Anderson et al. (1984) and Cadet and Daniel (1988) reached a similar conclusion after their more objective analyses of the period. The analysis upon which Fig. 6 is based suggested that the oscillation was present 58% of the time. Analyses of different variables can give slightly different results. For example, Knutson et al. (1986) presented a histogram generally similar to those of Fig. 6 but based on eastward-propagating anomalies in outgoing longwave radiation (OLR). However, they found a larger spread than in Fig. 6 with two cases having periods less than 20 days and two greater than 79 days, and concluded that the oscillation was present more than 75% of the time.

The period of the oscillation spans a wide range but it is separated from synoptic-scale variations (less than 10 days) and from seasonal variations. Its most frequent occurrence is near 45 days.

5. Clouds

We have seen that Gruber (1974) and Zangvil (1975) used space–time spectral analysis to show that there was evidence of eastward-propagating cloudy areas in the equatorial region with a wave 1 to wave 2 zonal scale. Zangvil also showed the eastward-moving clouds with a time–longitude section, and he demonstrated that they were most marked on the summer side of the equator.

Based on OLR measurements, Lau and Chan (1983) reported on a 2–3-month oscillation in clouds between Indonesia and the equatorial region at the date line, which they referred to as a dipole. In a subsequent paper, Lau and Chan (1986a, their Fig. 4) presented a map of the percent OLR variance contained in the 40–50-day period range based on seven 6-month segments from May to October. It showed that 12% of the variance was in the 40–50-day band over nearly the entire Indian Ocean north of the equator and also over the western Pacific from about 10° to 20°N. For a white noise process we would expect only 2% in this range. Weickmann et al. (1985) showed that spectra of OLR has significantly (95% level) more variance in the 28–72-day range than appropriate red noise spectra over regions in the central Pacific, equatorial eastern South America, and Africa, in addition to those over the Indian Ocean and western Pacific. Cross-spectral analyses (Weickmann et al. 1985) and lag correlation between points (Lau and Chan 1986a) revealed the eastward propagation of the OLR anomalies from about 60° to 160°E on these time scales.

Nakazawa (1988) studied the structure of the eastward-moving cloud masses with 3-h geostationary OLR data. He found that the eastward-moving cloud systems were composed of several eastward-moving super cloud clusters (SCC). Each SCC was, in turn, composed of smaller cloud clusters (CC) that moved westward. Each SCC has a scale on the order of 10^3 km and consists of a few of the CC whose scales are 10^2 km. The lifetime of the CC is only 1–2 days. New CC tend to form east of a fully developed CC. Figure 7 is a schematic taken from Nakazawa's paper. This behavior is confined to within 15° of the equator.

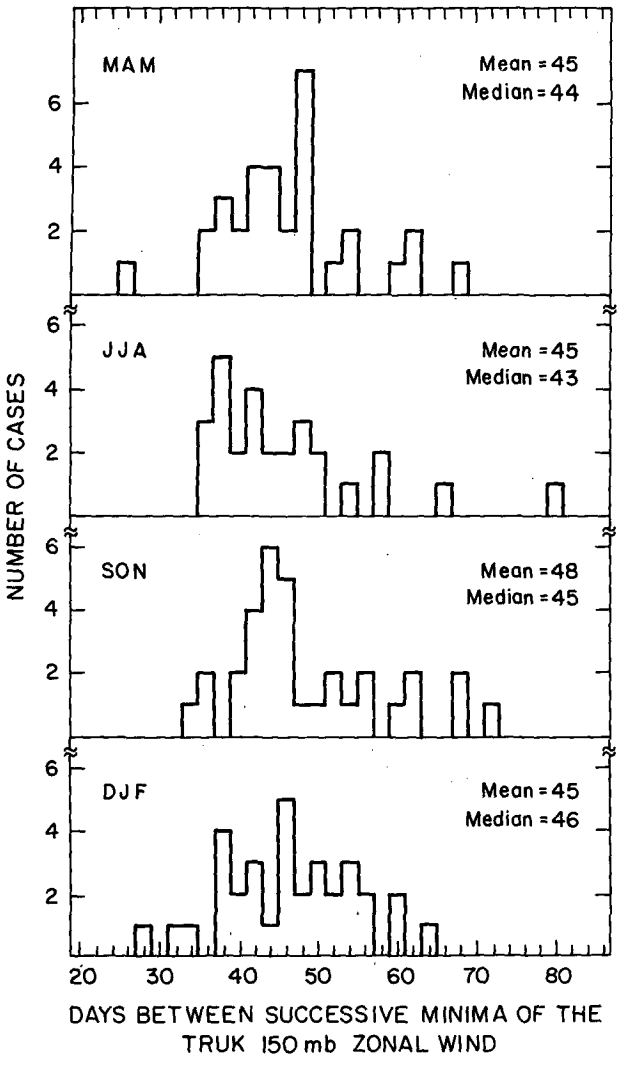

FIG. 6. Histograms of the observed periods based on subjective estimates of the time between successive minima of the 150-mb u at Truk (7.4°N, 151.8°E). Number of occurrences of 49- and 50-day periods is indicated at the point marked 50 and similarly at other points. The season for an occurrence is determined by the beginning date (from Madden 1986).

At 15° the cloud movement on all spatial scales tends to be westward.

But even near the equator there is additional complexity in the cloud systems beyond the SCC and CC. Further subtleties and variations in the cloud hierarchies were pointed out by Lau et al. (1991) and Sui and Lau (1992). Also, there are two regions where the eastward-traveling SCC are accompanied by local flareups of convection. They are near 100° and 150°E (Weickmann and Khalsa 1990). Khalsa and Steiner (1988) have studied the low-level (1000–700 hPa) precipitable water from the TIROS (Television Infrared Observation Satellite) Operational Vertical Sounder (TOVS) satellite instrument and they show stationary maxima in that quantity from October 1981 through December 1985 near 100° and 150°E. They point out that almost every occurrence of the precipitable water anomalies that exceed 38 mm in those two regions is accompanied by eastward-moving upper-level divergence as measured by the 250-hPa χ.

There are other interesting aspects of the large-scale cloud complexes associated with the oscillation besides the eastward propagation. We will see in a later discussion of monsoons that they are often related to the onset of the Indian and Australian summer monsoons. There are also the northward-propagating branches of the cloud systems over India and Southeast Asia. However, it should be noted that all large cloud complexes near the equator in the Indian and Pacific Oceans are not related to the eastward-propagating oscillation. Wang and Rui (1990) studied OLR data and have summarized various behaviors of large-scale tropical cloud complexes. They defined tropical intraseasonal convection anomalies (TICA) to have a minimum lifetime (four pentads), a minimum scale (30° of longitude), and a threshold anomaly strength or intensity (-15 W m^{-2}). At their strongest stage the TICA must be larger than 50° of longitude and their anomalies must be less than -50 W m^{-2}. Wang and Rui found 122 TICA during a 10-yr period (1975–85 with 1978 missing). Of those, the majority moved eastward (77), 27 moved northward with no connection to an eastward-moving TICA, and 18 moved westward. These last 18 were relatively weak as measured by their coldest OLR anomalies. This further emphasizes that while the schematic of Fig. 3 is representative of the oscillation near the equator, there are large-scale cloud complexes that behave differently. We point out that Cadet (1983) and Murakami (1984) also found westward-propagating cloud complexes, mostly west of 140°E.

We presume that the 77 eastward-propagating TICA are like Nakazawa's SCC and related to the oscillation. Wang and Rui divide them into three groups. The first, 32 cases, are equatorially trapped in that their centers stay within ±15° of the equator during their lifetime. Wang and Rui call them the EE mode. A second group, 25 cases, moves eastward along the equator but near 100°E begins a northeast (13 cases) or southeast (10 cases) movement, or in two cases splits with one part moving northeast and one moving southeast. These are called the NE and SE modes, respectively. The third group, 20 cases, combines eastward movement with northward movement over India and/or the western Pacific and are called the EN mode. Wang and Rui summarize the behavior of these three groups by determining the frequency of occurrence of each in 2° × 2° latitude–longitude squares, and their figure is reproduced here as Fig. 8. The different behavior in the TICA is clearly shown. Wang and Rui found that 78% (25 cases) of the equatorial eastward TICA (EE) oc-

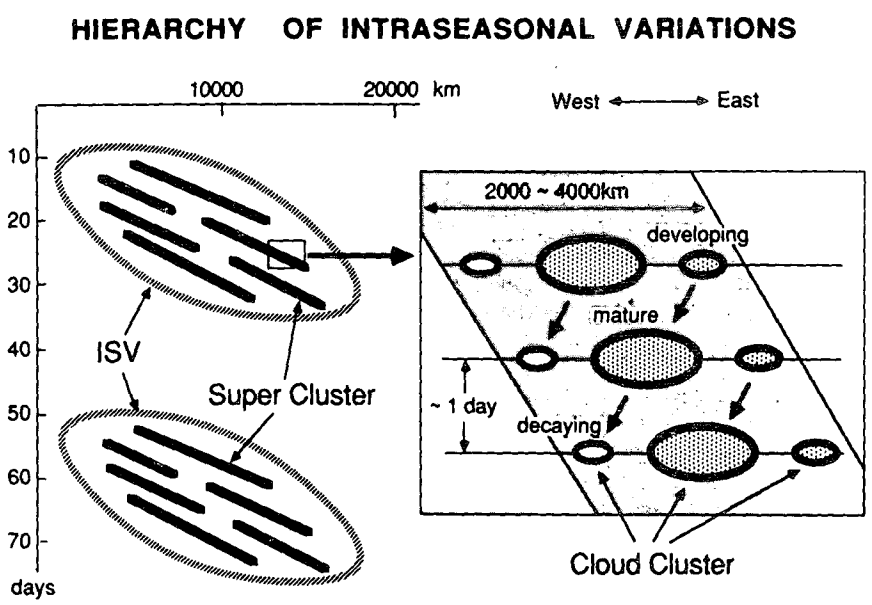

FIG. 7. Schematic describing the details of the large-scale eastward-propagating cloud complexes [slanting ellipses marked ISV (intraseasonal variability) on the left-hand side]. Slanting heavy lines represent super cloud clusters (SCC) within the larger complexes or ISV. The right-hand side illustrates the fine structure of the SCC with smaller westward-moving cloud clusters that develop, grow to maturity, and decay in a few days (from Nakazawa 1988).

curred during the 6-month period from December to May. Members of the second group that move to the southeast near 100°E (SE) occurred exclusively from November through April, indicating a relation to the ITCZ and Australian monsoon. Those that moved northeast (NE) occurred primarily, but not exclusively, in the northern summer, again associated with the ITCZ and the East Asian monsoon. The group that combined both northward and eastward (EN) movement took place most frequently in May and October. None was recorded during June through August, a time when independent northward-moving TICA were frequent. However, this is probably not always the case. We will see eastward- and northward-moving TICA, EN modes, during June and August of 1979 [Fig. 11 to follow, which is taken from Lau and Chan (1986a)]. We will also discuss Yasunari's work (1979) that documents EN-like clouds occurring during June to August 1973. This apparent discrepancy may be due in part to the fact that since TICA often span more than 1 month, Wang and Rui set the time of occurrence during the month when the TICA were at their maximum intensity.

Wang and Rui (1990) also documented the areas where the eastward-moving TICA formed. Their figure showing the results is presented here as Fig. 9a. The major formation region is the west-central equatorial Indian Ocean as predicted in Fig. 3. There is a secondary source just west of equatorial Africa. They also determined that the TICA tended to have the lowest OLR values in the region of the east-central Indian Ocean with a weak secondary region of low OLR along the equator near 160°E (Fig. 9b). These correspond to the regions of quasi-stationary pulsations discussed by Weickmann and Khalsa (1990). Wang and Rui (1990) showed that the maximum intensification rates of the TICA were in the central equatorial Indian Ocean, with secondary areas of intensification near 160°E north of the equator, and one extending from Australia to the date line south of the equator. Intensification occurs in the first secondary area during boreal summer and in the second during boreal winter, which is again consistent with these regions of intensification being coincident with the ITCZ (Wang and Rui 1990).

6. Monsoons

a. The Indian summer monsoon

Raghavan et al. (1975) showed a remarkable variation in precipitation over west coastal Indian stations from Vengurla (16°N) to Dahanu (20°N). There were large maxima 33 days apart on 7 July and 9 August 1962 with near zero precipitation in between. The low-level, northward-flowing wind over Kenya had corresponding fluctuations. Although there was some controversy over whether or not the Kenyan winds could be used to predict the Indian rainfall, Findlater (1969) argued that these same precipitation changes were in response to the changing Somali jet. The fluctuating

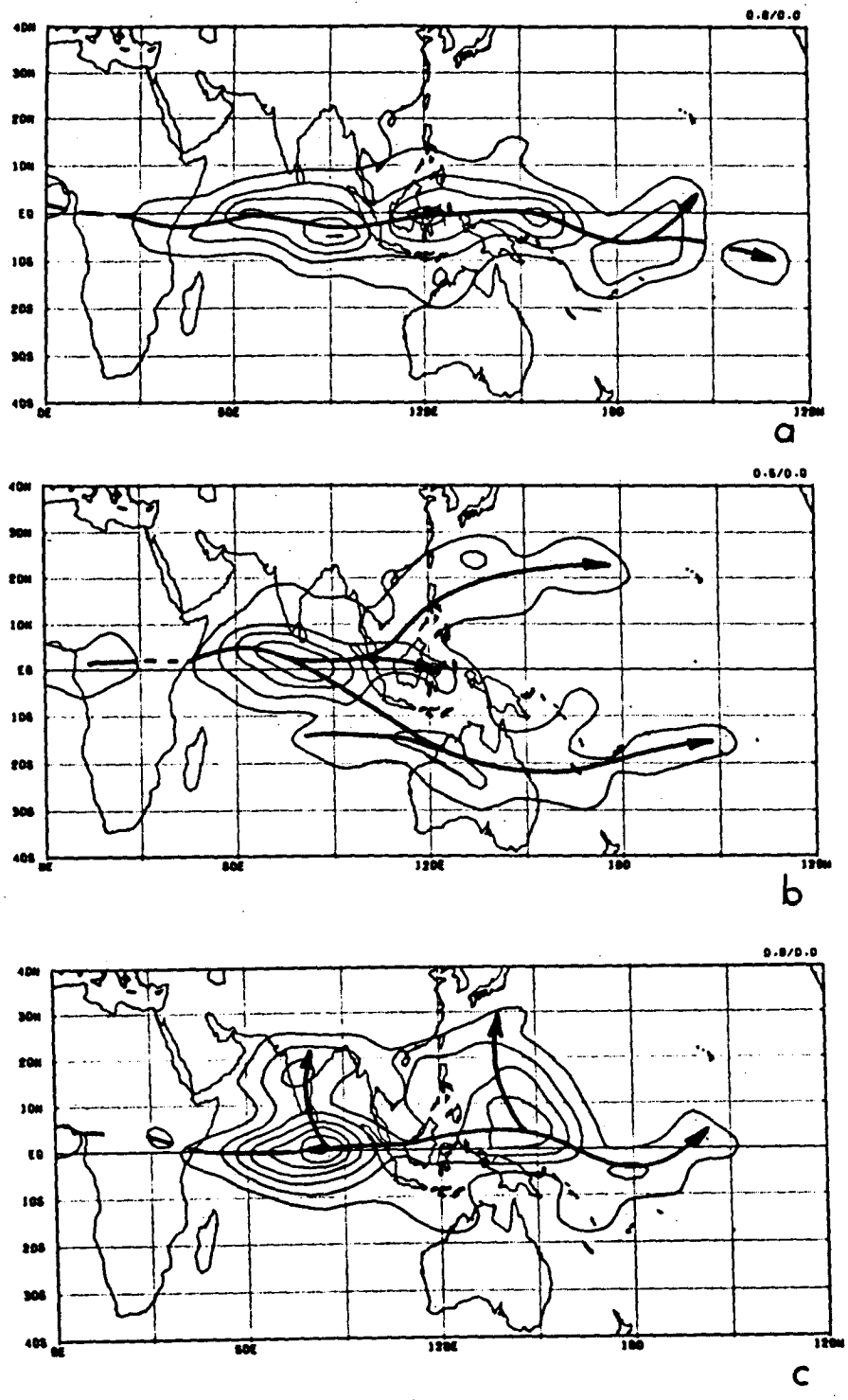

FIG. 8. Contour plot of the total number of occurrences of strictly eastward-moving cloud complexes (a); eastward complexes that split either to the north or to the south over the eastern Indian Ocean (b); and eastward-moving complexes that are connected with cloud systems that move northward into southern Asia (c); in each 2° × 2° box for a 10-yr period (1975–85, 1978 missing). The contour interval is 0.8 in (a) and (c), and 0.6 in (b). The heavy lines indicate the central paths (from Wang and Rui 1990).

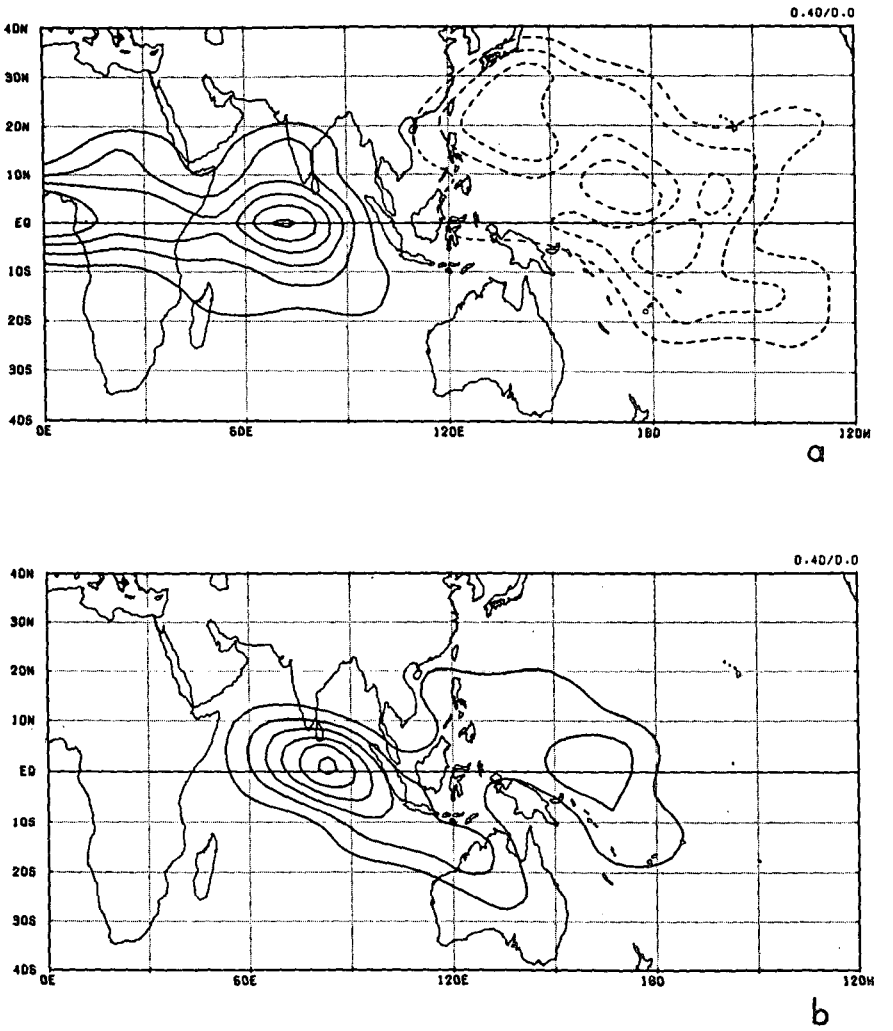

FIG. 9. Contour plots of (a) the total number of formations (solid) and terminations (dotted) of the eastward-moving cloud complexes, and (b) of the occurrence of the center, or location of lowest OLR value, at the strongest phase. Contour interval is 0.4. A spatial smoother has been applied to the basic counts (from Wang and Rui 1990).

Indian rains are called the "break" and "active" phases of the monsoon. Figure 10 is an example of the effects on Indian west coast precipitation of break and active phases during MONEX (taken from Cadet 1986). The break and active monsoon phases shown in Fig. 10 were accompanied by correspondingly small and large water vapor flux across the Arabian Sea (Cadet and Greco 1987).

Wylie and Hinton (1982) computed 10-day-averaged surface wind stress over the Indian Ocean during MONEX. They showed maximum values of 0.35 N m^{-2} in the region of the Somali jet over the western Arabian Sea in mid-June (their Fig. 7) before the onset of heavy rainfall over western India, and 0.60 N m^{-2} in late June coincident with it (their Fig. 9). Subsequently, the stress fell to 0.40 N m^{-2} through the first two-thirds of July during the monsoon break and then increased to 0.55 N m^{-2} in late July coinciding with the second active period shown by Cadet's figure. This is consistent with Findlater's (1969) and Raghavan et. al.'s (1975) suggested link between variations in large-scale surface winds and the Indian monsoon. Krishnamurti and Ardanuy (1980) also studied monsoon breaks and found associated large-scale pressure changes in addition to fluctuations in the Somali jet. In particular, space–time spectra indicated 30–40-day, eastward-propagating zonal wave 1 and 2 surface pressure oscillations, and that 30–40-day filtered pressure ridges passed India between 20° and 30°N about 5 days after a break.

It happens that the active monsoon periods are often connected with northward-moving cloud zones similar

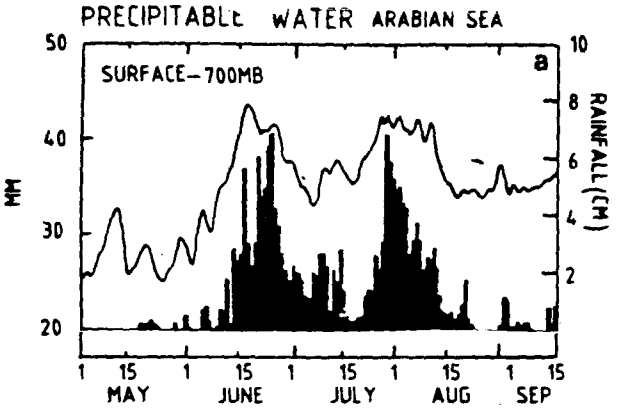

FIG. 10. Time series of the precipitable water from the surface to 700 hPa over the Arabian Sea (thin line) from *TIROS-N*, and the precipitation along the west coast of India during MONEX (adapted from Cadet 1986).

to those documented by Wang and Rui (1990). Murakami (1976), studying cloud data from eight June–September periods, used lag correlations to show that clouds associated with the active phases propagated northward through the Indian Ocean and Indian subcontinent at about 1° latitude per day. These northward-propagating clouds were oriented as northwest–southeast bands.

The first paper to directly relate eastward propagation of clouds near the equator and the northward propagating bands was that of Yasunari (1979). He presented a longitude–time diagram for the northern summer of 1973 that shows clouds propagating eastward near the equator from 60°E to 150°W. The longitudinal range is very similar to that suggested by the schematic of Fig. 3 and by the frequencies of occurrence documented by Wang and Rui (1990, and Fig. 8 here). He also presented a latitude–time diagram of cloudiness along the 72°–84°E longitude zone in which northward movement of the clouds is clear. From these two figures one could see that as the cloudy zone propagates eastward from 60° to 80°E, a part moves northward to 30°N. This is an example of one of Wang and Rui's EN modes.

The northward propagation was confirmed through studies of several Indian monsoons by Sikka and Gadgil (1980), Yasunari (1980, 1981), Krishnamurti and Subrahmanyam (1982), and Lau and Chan (1986a). Figure 11 is adapted from Lau and Chan (1986a) and shows the phenomena during MONEX. The two active periods shown in Fig. 10 correspond to the negative OLR anomalies shown in the left-hand panel of Fig. 11 that reach 15°N in mid-June and late July. The mid-June episode is clearly linked with eastward-moving clouds at 80°E and the equator (right-hand panel of Fig. 11). The late July episode is not clearly linked to eastward-moving clouds at 80°E and the equator but it does develop about the time of the passage of an eastward-moving upper-level velocity potential maximum and divergence as shown by Lorenc (1984), Krishnamurti et al. (1985), and Chen et al. (1988) and may be related to the eastward-moving clouds that are evident at 120°E in Fig. 11. The northward-propagating cloud zones often occur at approximately 30–40-day intervals. Indeed, Murakami's (1976) spatial correlations reach large negative values at lags of 16–20 days suggesting a period range of 32–40 days. To stress again the variability of the oscillation we point out that Mehta and Krishnamurti (1988) found regular *northward* propagation during the northern summers of 1979, 1982, and 1983 but not during the summers of 1980, 1981, and 1984. Interestingly, during the northern summers of 1980 and 1981, Knutson et al., (1986) still found regular *eastward* propagation of 250-hPa u-wind anomalies averaged from 0° to 10°S.

The relevance of the 40–50-day equatorial oscillations to the break–active phases of the Indian monsoon demonstrated by Yasunari renewed our interest. To further substantiate Yasunari's suggestion that the northward movement of cloudiness and the break and active phases of the monsoon might be related to the equatorial 40–50-day oscillation, we published composites of rainfall and cloudiness (Julian and Madden 1981) that showed the oscillation at Car Nicobar (9.2°N, 92.8°E) and Port Blair (11.7°N, 92.7°E) in the Bay of Bengal and at Minicoy (8.3°N, 73.0°E) just south of India (Fig. 12). The composites of Fig. 12 were based on the 150-hPa zonal winds at Truk Island over 6000 km to the east. When the 150-hPa zonal wind is a maximum (minimum), the precipitation and cloudiness is

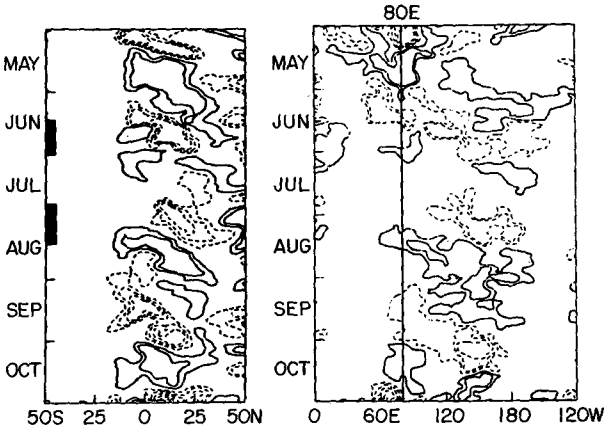

FIG. 11. Longitude–time section of anomalies in outgoing longwave radiation along the equator (5°S–5°N) during MONEX (right-hand side). Latitude–time section along 80°E (75°–85°E) for the same period (left-hand side). Contours are watts per square meter with negative values dashed and the zero contour suppressed. Times of active monsoon phases from Fig. 10 are indicated on the left-hand side by the dark bars (adapted from Lau and Chan 1986a).

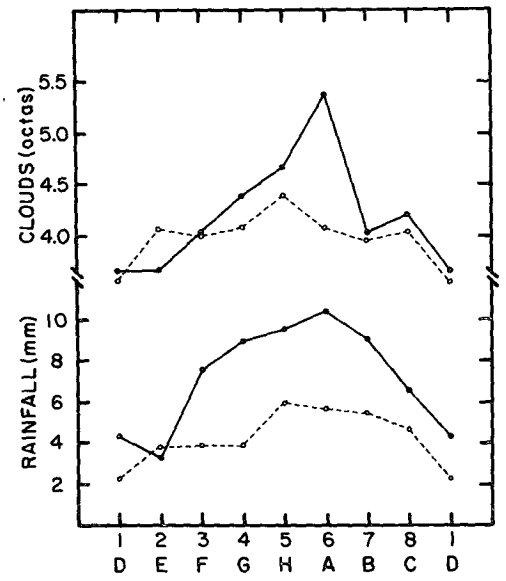

FIG. 12. Composited clouds and rainfall for Minicoy (8.3°N, 73.0°E) (dashed) and for Car Nicobar (9.2°N, 92.8°E) and Port Blair (11.7°N, 92.7°E) (solid). Letter phases are as in Fig. 3. Clouds are for the 5° × 5° latitude–longitude square over Minicoy and 10° × 5° latitude–longitude square over Car Nicobar and Port Blair. The numbers at the bottom correspond to times of specific 150-hPa u-wind anomalies at Truk (7.4°N, 151.8°E). Times 1 and 5 are those of minimum and maximum u wind, respectively (from Julian and Madden 1981).

a near maximum (minimum) over the Indian region consistent with a strengthening (weakening) of the circulation in the equatorial plane. The letters at the bottom of Fig. 12 approximately correspond to those of Fig. 3.

It appears that during the Indian summer monsoon clouds arrive from Africa or form in the equatorial Indian Ocean and then move both northward at about 1° latitude per day and eastward at 5° longitude per day on the 40–50-day time scale. Judging from Figs. 9a and 11, most frequently the clouds do not form very far south of the equator, but whether or not there are important influences originating in southern midlatitudes is an interesting question. Based on evidence from Tananarive (18.8°S, 47.5°W), Yasunari (1981) speculates that the origin of the clouds might be cold-air outbreaks from Southern Hemisphere midlatitudes. Murakami (1987) noted that when there was clear eastward propagation of disturbances along the equator there was also a strong cold surge from the southern midlatitude Indian Ocean at 850 hPa. While this evidence is intriguing, the role of southern midlatitudes in the active periods of the Indian summer monsoon remains unknown.

Further details of the behavior of these northward-moving cloud zones were presented by Hartmann and Michelsen (1989) in their study of rainfall data from 3700 Indian stations during 70 summer monsoons. They averaged data from all available stations in 1° squares and computed spectra. They found spectral peaks near 40 days over most of the southern half of India. A break in the monsoon over central India on this time scale usually occurred during a time of maximum near-equatorial precipitation indicating a meridional scale of the cloud zones of 1×10^3–2×10^3 km. These were times of equatorial westerlies and easterlies over southern India. As the equatorial 40–50-day low moves eastward, a trough progresses northward over India and westerlies and rain return initiating an active period. There are some smaller-scaled features that differ from this simple picture. For example, during a break, Hartmann and Michelsen found a maximum in precipitation in southeast India as easterlies north of the equatorial low release their moisture as they rise up the Ghat Mountains.

b. The Australian summer monsoon

Holland (1986) noted an average of 40 days between active bursts of the Australian summer monsoon. Undoubtedly some of these variations are related to the SE modes documented by Wang and Rui (1990). Hendon and Liebmann (1990b) showed that there was a pronounced 30–50-day modulation of monsoonal westerlies and that 27 out of 30 monsoon onsets from 1957 to 1987 coincided with the arrival of clouds associated with an eastward-propagating 40–50-day oscillation (Hendon and Liebmann 1990a). However, the poleward propagation of clouds that accompanies the major active periods of the Indian monsoon was not found. Hendon and Liebmann (1990a) pointed to an apparent poleward expansion of the clouds during active phases of the Australian monsoon rather than regular poleward progression. McBride (1983) reached a similar conclusion based on his analysis of the 1978/79 monsoon. Certainly, the SE modes of Fig. 8b are involved.

7. Effects in the extratropics

Some have argued that there may be a separate, midlatitude 40-day oscillation (Dickey et al. 1991; Ghil and Mo 1991a,b). Indeed, modeling studies indicate that there is an unstable global, barotropic mode with a 40-day period (Simmons et al. 1983). Also, Legras and Ghil (1985) have proposed that there may be instability caused by the interaction of the jet stream and mountain ranges at midlatitudes whose dominant period is near 40 days. Supporting the idea that there could be a 40-day midlatitude oscillation separate from the tropical one is the fact that the University of California, Los Angeles general circulation model is known to exhibit a 50-day variation in the relative atmospheric angular momentum without having the tropical 40–50-

day oscillation (Marcus et al. 1990). In addition, Magaña (1993) has observed small oscillations in the atmospheric angular momentum in the extratropics of 40 (Northern Hemisphere) and 50 days (Southern Hemisphere) that are apparently independent of any tropical activity.

Our purpose here is to describe only the tropical oscillation and any midlatitude manifestations that it may have. A disturbance that is of global scale longitudinally and that has such a profound effect on tropical convection, pressures, and circulation may also affect midlatitudes. Anderson and Rosen (1983) have shown that some of the 40–50-day variations in relative atmospheric angular momentum propagates up and out of the tropics to midlatitudes. Nevertheless, it is our contention that robust midlatitude responses are hard to find. That it is likely that the "average" response does not regularly occur due to the complexities of the ever-changing background flows of extratropical latitudes. This section describes some work on midlatitude variations thought to be related to the tropical oscillation, but we stress that any single event may not affect the midlatitudes in the described manner.

Weickmann (1983), Weickmann et al. (1985), Knutson et al. (1986), Knutson and Weickmann (1987), and Kiladis and Weickmann (1992) have described global aspects of the oscillation as they occurred in OLR and 250-hPa streamfunction and velocity potential. They show regular eastward propagation in the equatorial region of OLR and of velocity potential. In particular, the OLR anomalies follow the upper-level divergence and are strongest over the Indian and western Pacific Oceans, negligible over the cooler waters of the eastern Pacific and the Atlantic, and weak but present over South America and Africa. The OLR anomalies are also found to be strongest on the summer side of the equator. The zonal winds at 250 hPa propagate about 6 m s^{-1} from 40° to 160°E and then at 15 m s^{-1} from 160°E to the Greenwich meridian. When the clouds are in the Indonesian region the upper tropospheric flow tends to be characterized by twin anticyclones near the longitudes of the convection. To the east, twin cyclones were found. These anticyclones and cyclones extend roughly ±40° from the equator. Figure 13 is a schematic taken from Weickmann et al. (1985) for the 250-hPa circulation. [A more detailed picture is contained in Kiladis and Weickmann (1992), their Figs. 5 and 6.] This general picture is favored when the cloudiness is between 100° and 140°E and corresponds approximately to phase H or A of Fig. 3. Weickmann et al. point out that when the clouds push to the date line the upper-level circulation is approximately reversed from that of Fig. 13. This is also a time when an anomously clear region propagates eastward from 60° to 140°E and corresponds to phase D or E of Fig. 3. There is an expansion of the circumpolar vortex in regions of equatorial cloudiness and subtropical anticyclones and a contraction in regions of suppressed equatorial cloudiness and subtropical cyclones. Krishnamurti and Gadgil (1985) and Weickmann et al. (1985) showed that equatorial circulation anomalies are out of phase in the vertical but that poleward of about 20° they are in phase or equivalent barotropic.

During the May–October period, anomalous westerlies tend to occur at 850 and 250 hPa over southern Australia 5–10 days after the peak convective activity occurs in the western tropical Pacific (Knutson and Weickmann 1987). Graves and Stanford (1987) reported 45–53-day variations in the upper-tropospheric zonal winds over Easter Island (27.1°S, 109.3°W). These variations were strongest in June–August. They may be related to the changes in the 250-hPa westerlies over Australia, although they have not as yet been directly related to them nor to the equatorial oscillation.

Chen and Murakami (1988) have shown an interesting 40-day north to south oscillation of clouds along 140°E (longitude near Japan) north of 20°N during the northern summer of 1979. These are undoubtedly related to fluctuations in the east Asian monsoon or Meiyu over China (Baiu over Japan) documented by Lau and Chan (1986a) and Lau et al. (1988). There have also been published reports of 40–50-day spectral peaks in the winds south of Japan (Matsuo 1984; Kai 1985). Kai found these spectral peaks in surface winds over the Nansei Islands (25°–30°N). They are predominant in the northern summer and thought to reflect typhoon activity. There is some evidence that tropical cyclone formation may be related to the oscillation (Nakazawa 1986). A possible mechanism might be Ekman pumping in the boundary layer poleward of westerly surges associated with the oscillation, which would provide large-scale convergence favorable for typhoon and tropical cyclone formation.

Kousky (1985) shows variations in tropospheric thickness over the eastern United States. During the 1984/85 northern winter, positive thickness anomalies (ridging) over the eastern United States occurred when the 40–50-day convection shifted from the Indian Ocean to Indonesia. The opposite occurred when the convection approached the central Pacific. This seems to be consistent with the contracted and expanded circumpolar vortex of Fig. 13 over the United States (and its opposite) pointed to by Weickmann et al. (1985). Kousky's observations are based on only one season, so they must be considered with care. If such relationships stand up, they could offer some help in making long-range predictions for the United States.

8. Atmospheric angular momentum

Because the angular momentum of the earth–atmosphere–ocean system remains constant except for slow changes due to tidal influences, a change in the angular momentum of the atmosphere is reflected in opposite

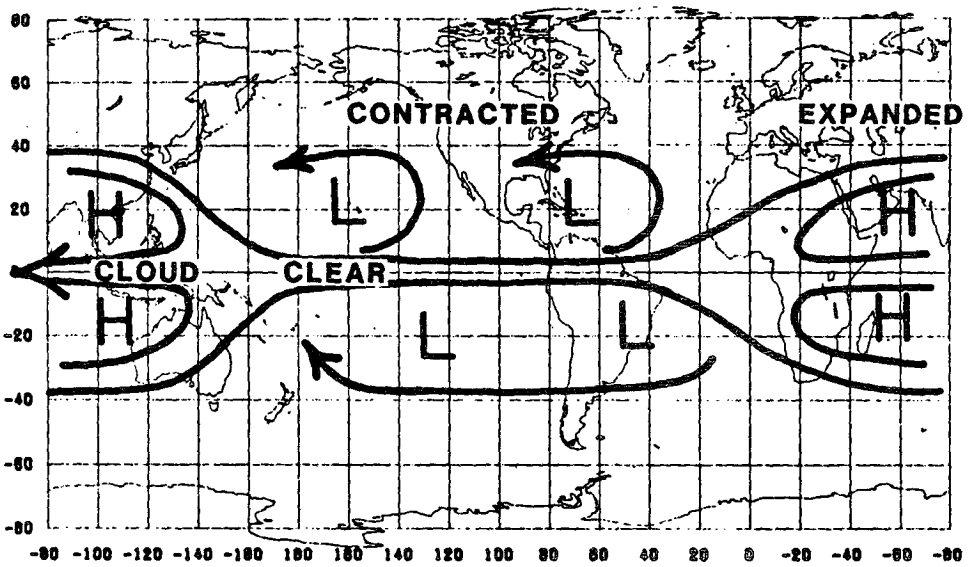

FIG. 13. Schematic of relationship between outgoing longwave radiation as signified by "cloud" and "clear" regions and the 250-hPa circulation at a time when maximum cloudiness is in the eastern Indian and extreme western Pacific Oceans (from Weickmann et al. 1985).

changes in the oceans or the solid earth. Munk and Miller (1950) and Frostman et al. (1967) showed that seasonal changes in the length of day (LOD), or rotation of the solid earth, could be explained by similar but opposite changes in the relative angular momentum (AAM) of the atmosphere. These changes are about 1 ms (10^{-3} s), with the longest days occurring during northern winter when the AAM exceeds that of the northern summer by about 6×10^{25} kg m^2 s^{-1}. For an up-to-date review, see Rosen (1993).

In 1974 Lambeck and Cazenave compared the LOD and AAM and found that changes in LOD on time scales less than six cycles per year were caused by changes in the AAM. They showed an oscillation in the AAM with a 50-day period from 20 February to 9 April 1968 (Lambeck and Cazenave 1974, their Fig. 5). Feissel and Gambis (1980) reported a 50-day period in the LOD during 1979, and Langley et al. (1981) documented the 50-day period in both LOD and AAM in a 4-yr period from 1976 through 1979. Spectra based on time series (1976–81) from Rosen and Salstein's continuing monitoring of the AAM have peaks near 50-day periods (Rosen and Salstein 1983). Gutzler and Madden (1992) showed that these peaks were the result of variations that occurred primarily from mid-January through September. An example of the AAM variation that occurred during MONEX is shown in Fig. 14. The amplitude of the oscillations about the smoothly varying seasonal trend is on the order of 10% of the total AAM and a few tenths of a millisecond change in the LOD.

Anderson and Rosen (1983) were the first to directly relate the 50-day AAM oscillations to the tropical oscillation. They showed that the zonal mean wind was correlated with the AAM on 45-day time scales from about 40°S to 60°N. The variations in the zonal wind seemed to originate in the upper troposphere of the equatorial region and move poleward and downward. When the upper-tropospheric zonal wind maxima moved poleward of 20°N and 20°S, the AAM reached its maximum (Anderson and Rosen 1983, their Fig. 8). The poleward propagation is shown nicely for the MONEX period by Magaña and Yanai (1991, their Fig. 13). Although there is coherence between zonal mean winds and AAM from 40°S to 60°N, Benedict and Haney (1988) and Gutzler and Madden (1993) showed the magnitude of the oscillations are such that, on average, nearly all of the contribution to the 50-day oscillation in the AAM comes from variations in the zonal winds between 20°N and 20°S.

By correlating the LOD with equatorial western Pacific surface pressures we were able to link indirectly the LOD and presumably AAM with the oscillation as it is depicted in Fig. 3 (Madden 1987). We concluded that the LOD and AAM reach their maxima when the convection associated with the oscillation is weakening over the central Pacific (between phase B and D of Fig. 3). During MONEX the relative maxima in AAM during late July and mid-August (Fig. 14) correspond with the time that convective anomalies have progressed at least to the date line (Fig. 11). This is also approximately the time of opposite phase or slightly before the

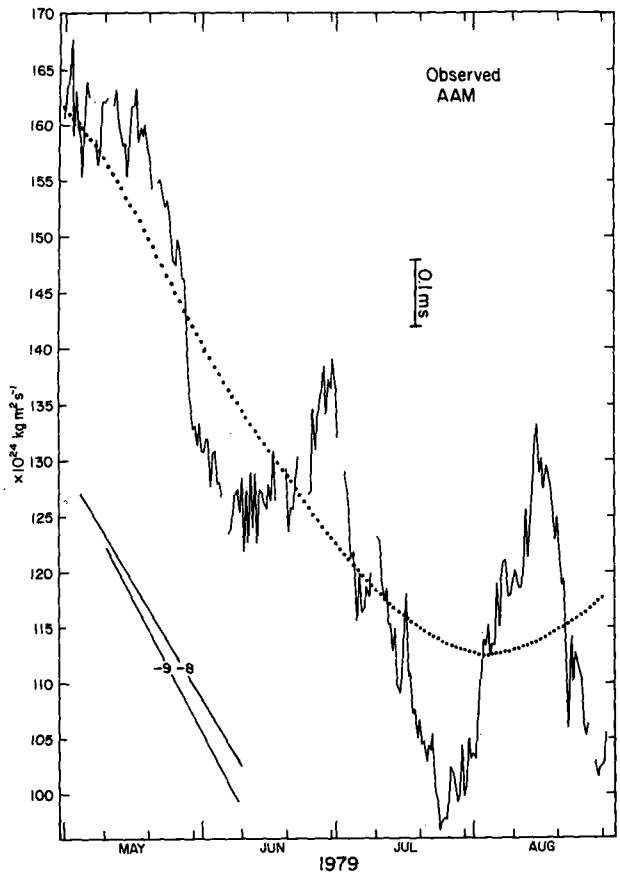

FIG. 14. Observed angular momentum of the atmosphere during MONEX taken from Rosen and Salstein (1983). Values at 0000 and 1200 UTC are plotted. Gaps reflect missing data. The dotted curve represents an approximate seasonal variation. The amplitude of a corresponding 0.1-ms change in the LOD is indicated. Sloping lines in lower left are the expected seasonal changes in AAM in units of 10^{18} kg m^2 s^{-2} based on torques computed from longer data records (Wahr and Oort 1984; Newton 1971) (from Madden 1988).

opposite phase of Fig. 13 (Weickmann et al. 1985). In addition, we showed that when convection was strong over the eastern Indian and western Pacific Oceans (phase H and A of Fig. 3) surface wind stress associated with a strengthening of the easterlies over the central Pacific could serve as the main mechanism increasing the AAM (Madden 1987, 1988; Kang and Lau 1990).

Weickmann et al. (1992) studied the AAM cycle during an oscillation. They found that minima in AAM occur when the convection is enhanced over the Indian Ocean and that a maximum increasing tendency of AAM occurs when the convection moves from the Indian to the Pacific Ocean. This agrees with our conclusions. However, their work indicated that the singular role of surface frictional stresses that we proposed is not correct during northern winter. At that time, they showed that surface wind stresses over the central Pacific are nearly out-of-phase with AAM. If they were the only driving force, the wind stresses would lead the AAM by 0.25 cycles. We computed the coherence and phase between AAM and the torque due to surface wind stresses over the equatorial belt from 28.9°S to 28.9°N for variations with periods of about 30–70 days over a recent 4-yr period (Madden 1992b). We found that during northern winter the wind stress torque leads the AAM by 0.4 cycles in good agreement with the out-of-phase (0.5 cycles) result of Weickmann et al. But from late July through October the wind stress torque leads AAM by 0.25 cycles, which is at least consistent with the possibility that it has the major influence on the AAM. Weickmann et al. (1992) also found the 0.25-cycle relationship during the May–September period.

Thus, fluctuations in tropical wind stresses associated with the oscillation are large and likely play an important role in forcing the oscillations in AAM, but it is necessary to study global frictional stresses and mountain or pressure torques to evaluate the oscillation's AAM budget. Weickmann and Sardeshmukh (1994) computed frictional and mountain torques for December 1984 and January 1985. Their sum was in good agreement with the AAM tendency during a 45-day oscillation. Weickmann and Sardeshmukh (1994) showed that during this oscillation the frictional torque and mountain torques contributed about equally. The frictional torque reached positive anomaly values first, about the time of largest negative anomaly AAM, in concert with an out-of-phase relationship during that season. About 10 days later, anomaly mountain torques were at their maximum. In this connection, Ghil (1987) has argued that extratropical mountain torques may be an important contributor to the oscillation. The fact that Anderson and Rosen (1983) have shown that anomalies in AAM propagate poleward also points to a role for extratropical torques. Mountain torques and frictional stresses over land are difficult to estimate, but it is clear that they will have to be considered in order to reach a full understanding of changes in AAM during the oscillation.

9. The seasonal variation

There is some seasonal variation in the oscillation associated with its roles in the Indian and Australian monsoons. Also, researchers have found that the oscillation's cloud activity favors the summer hemisphere and the general location of the ITCZ (Zangvil 1975; Wang and Rui 1990; Weickmann et al. 1985; Knutson et al. 1986), a result that is also at least partly related to the monsoons. We have seen that the average period of the oscillation shows no large change with season. There is, however, some change in strength as measured by the vertical shear in the u winds at Truk (Anderson et al. 1983; Madden 1986). Figure 15 is pre-

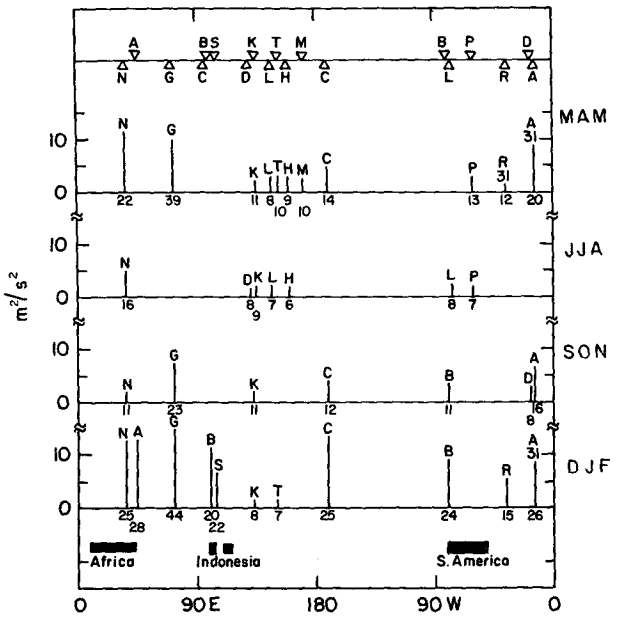

FIG. 15. Summary of the filtered 150-hPa u-wind variance at 19 equatorial stations. Longitudes of the stations are indicated by their initial and by the triangles along the top line. All stations are within 14° of the equator. Initials and triangles above (below) the line are for stations north (south) of the equator. The four lines below contain the results for northern spring (March, April, and May—MAM), summer (June, July, and August—JJA), autumn (September, October, and November—SON), and winter (December, January, and February—DJF). Vertical bars are included during a season for each station whose 47-day filtered variance exceeds that of its 31- and 99-day filtered variances. This situation reflects a spectral peak at 47 days. The number below a bar is the value of the 47-day filtered variance, and the length of the bar indicates how much that variance exceeds the average of the adjacent bands (left-hand scale). At Ascension Island (8.0°S, 14.4°W) and Recife (8.1°S, 34.9°W), variance in the 31-day band sometimes exceeded that in the other bands. Those cases are indicated and there the bar and number represents 31-day variances. The longitudes where land masses intersect the equator are indicated at the bottom.

sented to further illustrate seasonal changes in the oscillation as measured by the 150-hPa u wind at tropical stations. It is taken from Table 2 in Madden (1986). The horizontal axis represents a zonal cross section along the equator. The line at the top indicates the longitudinal location of the 19 stations that were studied. The u winds from these stations were bandpass filtered with three slightly overlapping filters centered at 1/99, 1/47, and 1/31 day. The half-power bandwidth of the filters was about 1/100 day. The variance in each band was computed separately for each season. A vertical bar is present at a station if the 47-day variance exceeds that in the other two bands. The numbers below the bars indicate the total variance in the 47-day band, and the length of the bar indicates how much it exceeds the average variance of the other two bands. By these measures the oscillation is largest during December–February and smallest during June–August. It is smallest at stations in the western Pacific and largest at stations in the Indian Ocean and at Canton and Balboa. Similar conclusions were reached by Gutzler and Madden (1989). It should be noted that the 47-day variance that exceeds the average variance of the other two bands (i.e., that which exceeds a smoothly varying spectrum) ranges from only a few percent to 15% (at Canton and Balboa during December, January, and February) of the total daily variance [deduced from Table 2 of Madden (1986)].

A feature of the oscillation specifically related to the vertical shear is the tendency for the u wind to be coherent and out-of-phase between the lower and upper troposphere over the tropical Pacific and Indian Oceans. We found that that feature had an interesting seasonal variation (Madden 1986). Figure 16 shows the average coherence at 47-day periods between the 850- and 150-hPa u wind at Koror (7.3°N, 134.5°E) and at Darwin (12.0°S, 130.9°E). The phase angles are not shown but they indicate an out-of-phase relationship all year at Koror and during the time of maximum coherence at Darwin. We interpret seasonal variations

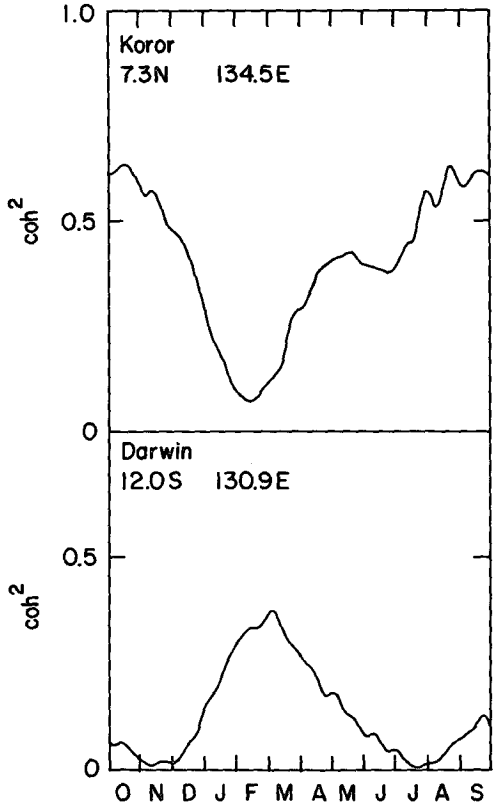

FIG. 16. Seasonally varying coherence squared between the 850- and 150-hPa u winds at Koror (7.3°N, 134.5°E) (top) and at Darwin (12.0°S, 130.9°E) (bottom) at 47-day periods. Time runs from October through September (from Madden 1986).

such as these that occur at stations in the Indian and western Pacific Oceans to result from the seasonal migration of convection associated with the ITCZ. The ITCZ is farthest south during northern winter, and the vertical coherence between the u winds is biggest at Darwin and other Southern Hemisphere stations at that time. The opposite is true during northern summer. [See Fig. 7 of Madden (1986) for coherence at other stations.]

We originally thought the lack of coherence between the u and v winds was a characteristic of the oscillation (Madden and Julian 1971). In fact, upper-tropospheric u and v are very coherent in the 40–50-day range at stations from at least Gan eastward to Balboa. This coherence, however, is revealed only by seasonal statistics. The reason is that u and v tend to be in phase during northern summer and out of phase during northern winter. Figure 17 contains the coherence at 47-day periods between u and v at 150 hPa over Singapore as a function of time of year. The maximum in coherence from December through April is associated with an out-of-phase relation, while that from June through October reflects a very nearly in-phase relation. Because of this seasonal phase change, cospectra (and coherence) based on time series that extend across seasons tend to be near zero.

This seasonal change in the phase relationship between the u and v winds is related to the seasonal change in the climatological winds. During northern winter the upper flow over the equatorial Indian and western Pacific Oceans is primarily from the southeast, while it is from the northeast during northern summer. The eastward-moving clouds associated with the oscillation cause a strengthening and weakening of the mean flow as they pass. As a result, there are fluctuations in the upper-level climatological northward transport of momentum (u and v in phase) across the equator during northern summer and in the southward transport there (u and v out of phase) during northern winter.

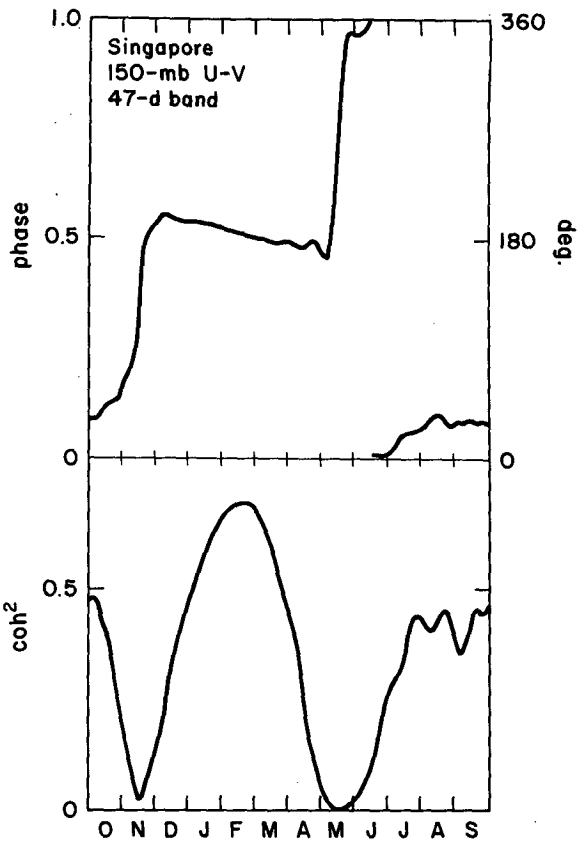

FIG. 17. Seasonally varying coherence squared (bottom) and phase (top) between 150-hPa Singapore u and v winds at 47-day periods. Phase between 0.0 and 0.5 cycles means that u leads v (from Madden 1986).

10. Oceans

Along with the surface wind stress variations over the Arabian Sea (Wylie and Hinton 1982) and the Pacific Ocean (Madden 1988), we should expect the effects of the oscillation to be manifest in the underlying seas. Lau and Chan (1985, 1986b) proposed an atmosphere–ocean interaction as a possible link between the oscillation and the onset of the El Niño. Krishnamurti et al. (1988) found sea surface temperature variations on 30–50-day time scales on the order of 0.5°–1°C, with the strongest variations occurring over the equatorial western Pacific Ocean and the Bay of Bengal. They also studied sensible and latent heat fluxes between atmosphere and ocean. In particular, during MONEX, the surface u wind over the Bay of Bengal (11°N, 90°E) has relative maxima in late May, late June, and early August (Krishnamurti et al. 1988, their Fig. 11). The latter two dates are ones of heavy rainfall over western India (Cadet 1986), strong winds over the Arabian Sea (Wylie and Hinten 1982), and strong winds over the entire tropical Pacific (Madden 1988). There are fluctuations in the latent heat flux at the surface over the Bay of Bengal too. Their amplitudes are roughly 40 W m^{-2} or about 20% of the average of 200 W m^{-2} there (Krishnamurti et al. 1988, their Fig. 11). It is clear that the exchange of heat between ocean and atmosphere is affected significantly. In addition, there is evidence for dynamic responses in the ocean to the winds of the oscillation and some of those follow.

a. Locally forced responses

McPhaden noted that low-level zonal winds at Gan Island were coherent and in phase with ocean currents to a depth of 100 m in the vicinity at 30–60-day periods (McPhaden 1982). The mixed-layer depth and the upper-thermocline temperature are similarly related to the wind. This is an example of the oscillation's wind vari-

ations driving similar variations in the upper ocean. Another one is the Somali Current off Kenya. Mysak and Mertz (1984) present evidence of a 40–60-day oscillation in the long-shore current and temperature off the Kenyan coast. They conclude that this oscillation is driven by the wind stress or the wind stress curl there. They offer further evidence to support this conclusion with an examination of the surface wind stress over the western Indian Ocean during January–October 1976 and January–September 1979 (Mertz and Mysak 1984). At the equator and 48°E, a spectrum of the v wind stress has no excess power in the 40–60-day band during the 1976 period but the u wind stress does. The wind-stress curl also has a spectral peak near 40 days. During 1979 both the u and v wind stresses have broad spectral peaks in the 40–50-day range. Another possible example of locally forced ocean responses to the 40–50-day oscillation are 50–80-day fluctuations in the current in the Arabian Sea (16°N, 60°E) during the May–September period of 1986 (Shetye et al. 1991). Composites of low-level winds associated with the 40–50-day oscillation indicate a relatively strong signal there, so local forcing is possible (e.g., Murakami 1984). More evidence for local forcing is found in Cadet (1986), who found 50-day peaks in spectra for the 850-hPa u wind over the Arabian Sea east of 50°E.

b. *Remotely forced responses*

Not all of the ocean responses to the low-level winds of the oscillation are local. The remarkable 40–60-day variations in sea level height (SLH) that Enfield (1987) has shown to exist from at least Callao, Peru (12°S), in the south to San Francisco in the north during the 1979–84 period is the leading example. Luther (1980) reported 35–80-day spectra peaks in SLH from Canton to the Galapagos Islands, and Enfield (1987) shows relatively high coherence and a nearly linear change in phase across a broad frequency range between the SLH at Nauru in the west-central Pacific and Talara (81°W) on the coast of Peru. The linear change of phase with frequency that he found is characteristic of a constant time delay between the two stations and a constant phase velocity. The phase velocity was eastward at about 2.9 m s^{-1} along the equator, which is consistent with that expected for the first internal-mode Kelvin wave (Enfield 1987).

Apparently these Kelvin waves are excited west of the date line where the low-level winds have considerable power in the 40–50-day range. They propagate at 3 m s^{-1} eastward and then poleward along the west coast of the Americas. Erickson et al. (1983) showed a coherence peak at 40-day periods between winds at Boru Island (1.3°S, 171.0°E) and an ocean pressure gauge at Isabela Island (0.0°S, 91.5°W) with a lag of 43 days, which corresponds to a propagation velocity of 2.9 m s^{-1}. Also, Enfield and Lukas (1984) found that when winds at 170°E are offset by 50 days, most of the prominent features of the winds are aligned with the SLH at Callao consistent with a propagation just under 3 m s^{-1}. Peaks in the spectra of SLH and bottom pressure that may relate to these Kelvin waves have been found during various time periods and at several longitudes in the equatorial Pacific (Mitchum and Lukas 1987; Chiswell et al. 1988).

c. *Other ocean variations*

There have been a number of reported 40–50-day variations in the ocean that cannot be clearly linked to the atmosphere oscillation. Quadfasel and Swallow (1986) found a dominant 50-day period in currents just north of Madagascar during the first half of 1975. Schott et al. (1988) reported that 41% of the variance in the transport was accomplished by 40–55-day time scales in a nearby region from October 1984 to September 1985. They pointed out that there were no similar local wind variations on that time scale, and attributed the ocean variability to shear instabilities in the mean flow. This conclusion is supported by the fact that ocean models of the region generate 50-day oscillations when forced only by monthly mean winds (Kindle and Thompson 1989; Woodberry et al. 1989). Kindle and Thompson attributed these variations to barotropic instability associated with the East African Coastal Current as an alternative to direct wind forcing. In the Gulf of Guinea (West Africa), Picaut and Verstraete (1976) found 40–50-day variations in sea surface temperature and height, which they tentatively ascribed to a resonant mode responding to local atmospheric variations.

11. The oscillation during MONEX

The oscillation was active during the entire FGGE year (e.g., Lorenc 1984). In particular, during the May–September period we have seen rainfall variations on the west coast of India (Cadet 1986, Fig. 10 here), associated clouds (Lau and Chan 1986a, Fig. 11 here), and AAM (Madden 1988, Fig. 14 here). There have been numerous studies of the oscillation during that time and some of their results for the MONEX underscore the very large scale effects of the oscillation.

The northward-propagating cloud zones that move over India (Fig. 11) were accompanied by similarly propagating cyclonic vorticity zones, low pressure and convergence in the lower troposphere, and anticyclonic vorticity and divergence aloft (Krishnamurti et al. 1985; Mehta and Ahlquist 1986; Chen et al. 1988). The upper-level divergence was related to the large-scale (zonal wave 1–2), eastward-propagating χ field (Lorenc 1984; Krishnamurti et al. 1985; Nogues-Paegle and Mo 1987; Chen et al. 1988).

During the period 21–27 June, when the Indian monsoon was active (Fig. 10), Murakami et al. (1984)

show at least three major cyclonic synoptic disturbances in the cyclonic vorticity zone that extended west-northwest to east-southeast from the Arabian Sea to approximately 135°E. This is consistent with the northward-propagating clouds along 80°E and the eastward-propagating ones along the equator documented by Lau and Chan (1986a) (and Fig. 11 here). Murakami et al. (1984) noted that the synoptic disturbances moved toward the northwest along the trough line while the line itself moved northward and eastward. (These off-equator, westward-moving disturbances have a longer time scale and somewhat bigger space scale than the CCs reported by Nakazawa.) This case is a good example of the equatorial oscillation's relation to active and monsoon break periods. It is an EN (eastward and northward moving) cloud mode defined by Wang and Rui (1990). Another manifestation of a similar trough line associated with an EN mode was that during 29 August–2 September of 1976. Wang and Rui (1990) showed that a narrow band ($1-2 \times 10^3$ km) of OLR anomalies less than -15 W m^{-2} extended from India east-southeastward to the equator at 150°E, during that 5-day period. Krishnamurti et al. (1985) found a similar orientation in the 30–50-day filtered 200-hPa χ field during active monsoon phases on 24 June and 29 July 1979 (their Fig. 5).

Figure 18 shows the surface wind stress over the Pacific during an active (20 June) and a break (10 July) period of the Indian monsoon. Positive wind stress means a transfer of eastward momentum from the earth to the atmosphere and occurs where the surface winds are easterly ($u < 0$). During the active phase (20 June) the wind stress is greater than that during the break (10 July), particularly in the 10°–30° latitude bands both north and south of the equator. During the active phase, the subtropical anticyclones were strong over the Pacific in each hemisphere resulting in a broad band of relatively strong easterlies from 30°S to 30°N (Fig. 18a). During the break phase, the subtropical anticyclones were weaker and midlatitude troughs extended north of 20°S east of Australia and near 130°W in the South Pacific, and south of 30°N at about 140°E and 140°W in the North Pacific (Fig. 18b). Krishnamurti and Subrahamanyan (1982) have remarked on the circulation change near 20°N, 140°E, south of Japan, with anticyclonic low-level flow present there on 19 June (active phase) and cyclonic flow there on 10 July (break phase), which is reflected in the change from westerly to easterly winds there (upper left-hand corners of Figs. 18a,b). The overall strengthening and weakening of the northern subtropical high with a roughly 45-day period is revealed by the remarkable, unfiltered (in time) time series of the 850-hPa height averaged over the region 25°–45°N and 180°–130°W discussed by Chen (1987). It has minima in the height before the monsoon, during the break, and after its retreat in early June, near 10 July, and late August, respectively. Maxima occur in late June and early August during the monsoon active phases.

We have already seen that extrema in the surface wind stress vary from 0.60 N m^{-2} to 0.40 and back to 0.55 N m^{-2} over the Arabian Sea during these same active and break phases (Wylie and Hinton 1982). It should be noted that these latter wind stress variations have opposite sign of those over the Pacific. Madden (1988) shows that it is the stresses over the Pacific that dominate and explain nearly all of the 40–50-day anomalies in the tropical (32°S–32°N) frictional torques.

It seems that the entire Pacific–Indian Ocean circulation pulsates with the oscillation. This pulsation is seen in the composites of the 850-hPa winds of Murakami (1984) during the period. Also, Chen (1985) studied the energetics in the tropics during MONEX and found large 45-day oscillations in eddy available potential and kinetic energy. Both had maxima during, or a few days after, the most active monsoon phases in late June and early August. These maxima were nearly a factor of 2 larger than the minima before monsoon onset, during the July break, and after monsoon retreat. Chen also showed a very large variation in the large-scale (zonal wave 1) momentum transport along 10°S in the upper troposphere with premonsoon (1–10 June) values near zero, active phase values of 31 and 58 m^2 s^{-2} (21–30 June and 1–10 August, respectively), and break (13–20 July) and postmonsoon retreat (22–31 August) values of 9 and 0 m^2 s^{-2}. Undoubtedly the in-phase oscillations of 150-hPa u and v during northern summer at Singapore revealed in Fig. 17 are a part of these large-scale variations.

Figure 18a (20 June) corresponds to phases H or A in Fig. 3 and to the upper-air schematic of Weickmann et al. (1985, Fig. 7) (Fig. 13 here). Comparing Fig. 18a and Fig. 13 we can see the baroclinic structure of the wind anomalies over the equatorial Pacific (strong easterlies near the surface and westerlies aloft) and the barotropic structure poleward of about ±20° (predominately strong easterlies at the surface and easterlies aloft). Comparing Fig. 18b corresponding to phases D or E of Fig. 3 and the opposite upper-air pattern of Fig. 13 reveals a similar equatorial baroclinic structure and extratropical barotropic structure. That is, the surface easterlies are now (10 July) less strong everywhere and are overlaid by anomalous easterlies near the equator and westerlies poleward of ±20°.

Table 2 is presented to relate the approximate timing of some of the phenomena observed during MONEX with the schematic of Fig. 3 for the oscillation in the equatorial plane and with that of Weickmann et al. (1985 Fig. 7) for the upper-level extratropics.

12. Discussion

Initial observational studies pointed out similarities in the oscillation's structure to that of an atmo-

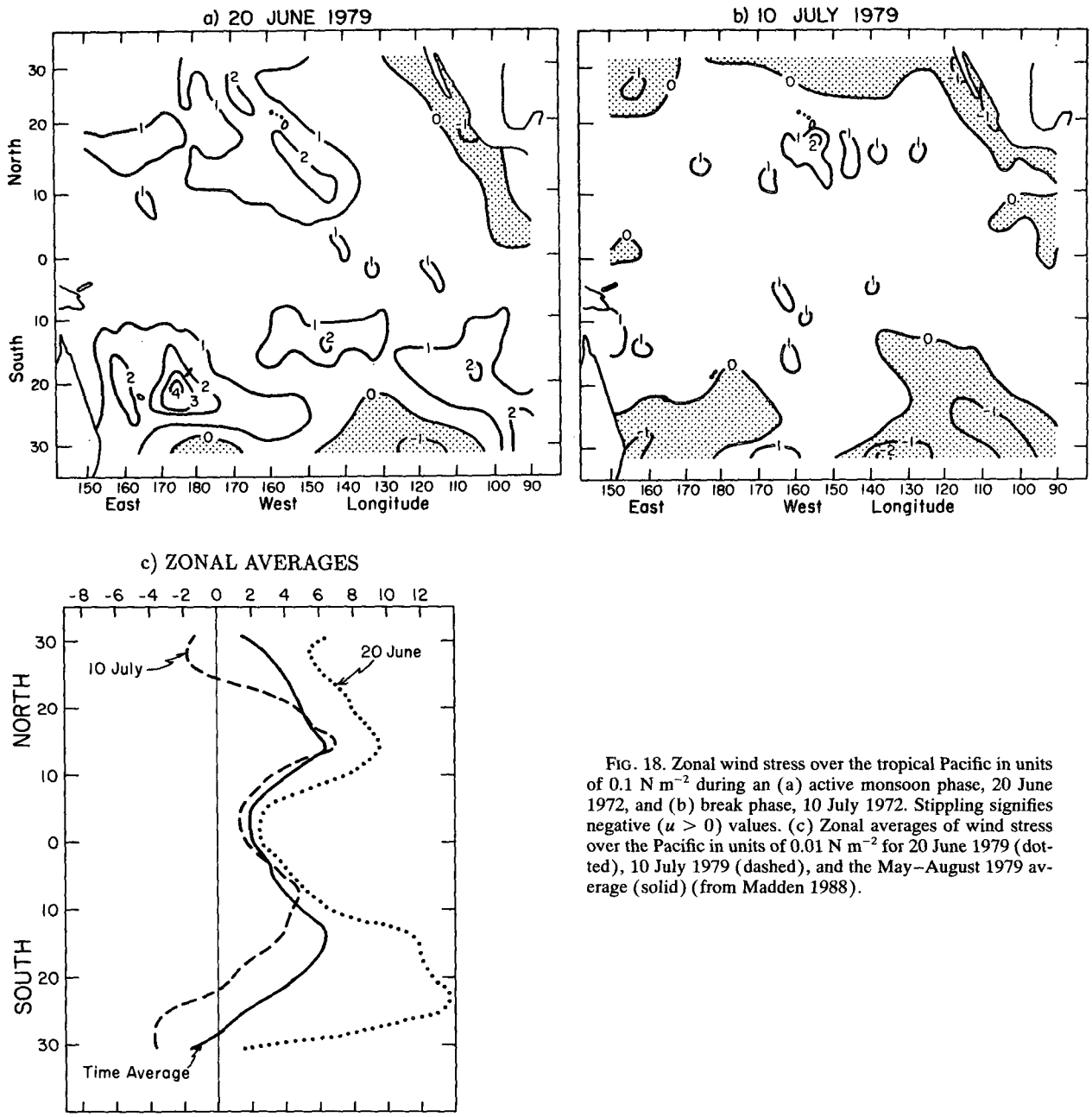

FIG. 18. Zonal wind stress over the tropical Pacific in units of 0.1 N m^{-2} during an (a) active monsoon phase, 20 June 1972, and (b) break phase, 10 July 1972. Stippling signifies negative ($u > 0$) values. (c) Zonal averages of wind stress over the Pacific in units of 0.01 N m^{-2} for 20 June 1979 (dotted), 10 July 1979 (dashed), and the May–August 1979 average (solid) (from Madden 1988).

spheric Kelvin wave (Madden and Julian 1971; Parker 1973). There were some early modeling and theoretical work that further suggested the possible role of the theoretically predicted Kelvin wave. For example, Holton (1973) found a maximum Kelvin wave response to white-noise forcing in the tropical upper troposphere at periods longer than 30 days in his linear, primitive equation model. There was a problem, however, because the Kelvin wave speed is proportional to its vertical scale, and the relatively large vertical scale of the observed oscillation would result in a propagation speed larger than observed. On the other hand, Lindzen (1974a,b) pointed out that wave-CISK (conditional instability of the second kind) indicated a 10-m equivalent depth for the tropical troposphere, which would be consistent with the observed slow speed. Another possible reconciliation between the observed, large vertical scale and the slow phase speed could be provided through the inclusion of viscous damping as was shown by

TABLE 2. Approximate timing of oscillation phenomena during MONEX with respect to that of the schematics of Fig. 3 and Fig. 7 in Weickman et al. (1985) (Fig. 13 here); A_E and K_E denote eddy available potential energy and eddy kinetic energy, respectively.

	Symbolic dates from Fig. 3.							
	F	G	H	A	B	C	D	E
Indian Monsoon			active				break	
Tropical A_E and K_E			maximum				minimum	
Low-level wind and water vapor flux over Arabian Sea			maximum				minimum	
Subtropical low-level anticylcones over Pacific			strong				weak	
Atmospheric angular momentum		minimum				maximum		
Frictional torque			maximum				minimum	
Extratropics from schematic of Weickman et al. (1985)			Fig. 13				opposite Fig. 13	

Chang (1977). In any case, exploration of the Kelvin wave was promising.

Yamagata and Hayashi (1984) examined the possibility that the structure of the oscillation is that of the response of the tropical troposphere to localized heating. They forced the model of Gill (1980) with periodic, 40-day heating. The solution consists of a Kelvin mode and Rossby modes to the east and west of the heating, respectively (Yamagata and Hayashi 1984; Gill 1980). Yamagata and Hayashi noted that, near the equator, the u wind and the pressure perturbations of the Kelvin mode are nearly in phase, while those of the Rossby mode response are nearly out of phase. Since Canton and Majuro are nearly always east of the main convection, the observed relations between u and pressure in the lower troposphere are consistent with this model (Nishi 1989, and Table 1 here). The same cannot be said about the more nearly out-of-phase character of u and z above 500 hPa at Canton and Majuro. Madden (1986) interpreted the high coherence between u and v shown in Fig. 17 as reflecting the presence of asymmetric Rossby waves near, or west of, the major convection. While we think that the coupled Kelvin–Rossby mode model serves as an adequate first-order model, it leaves many aspects of the oscillation unexplained. Besides the out-of-phase character of u and z in the upper troposphere, the schematic of the structure east of the convection shown in Weickmann et al. (1985) and here as Fig. 13 differs from that of an equatorial Kelvin wave.

We have surveyed most of the more recent theoretical and modeling papers addressing the oscillation. They all agree on the critical importance of moist processes to explain it, and from the empirical evidence this agreement is totally warranted. How the moist processes enter into any theoretical model is an important aspect but that is beyond any critical comment we might make. There is a feature of the descriptive material that we feel has not been given enough attention or comment, possibly for good reason. It is the presence of the mean zonal manifestation of the oscillation. However the zonal and meridional scale of the phenomenon is decomposed in theory (e.g., in zonal wavenumber), it should be remembered that the mean zonal structure (wavenumber 0) is present in several variables. This would seem to be an important feature to be explained. It also would seem to be the simplest nonphysical explanation of the coherence with the AAM and LOD quantities. Anderson and Stevens (1987) did study mean zonal modes in a zonally symmetric model. They suggested that the oscillation may result from the combined effects of zonally symmetric modes and asymmetric traveling modes.

The 40–50-day oscillation has provided fertile ground for research by empiricists, theoreticians, and modelers. Much is still to be learned. The oscillation is an important part of the general circulation, and because of its relatively long time scale, may help long-range forecasts (Cadet and Daniel 1988; Krishnamurti et al. 1990; Ferranti et al. 1990; von Storch and Xu 1990). It is clear that as understanding of the oscillation continues to improve so will the understanding and long-range prediction of weather and climate.

Acknowledgments. We thank T. N. Krishnamurti for encouraging us to write this review. D. Cadet, K.-M. Lau, H. Lejenäs, H. van Loon, B. Wang, and K. Weickmann provided helpful comments on an earlier version. J. Martin patiently and skillfully typed several drafts.

REFERENCES

Anderson, J. R., and R. D. Rosen, 1983: The latitude–height structure of 40–50 day variations in atmospheric angular-momentum. *J. Atmos. Sci.*, **40**, 1584–1591.

——, and D. E. Stevens, 1987: The presence of linear wavelike modes in a zonally symetric model of the tropical atmosphere. *J. Atmos. Sci.*, **44**, 2115–2127.

——, ——, and P. R. Julian, 1984: Temporal variations of the tropical 40–50 day oscillation. *Mon. Wea. Rev.*, **112**, 2431–2438.

Benedict, W. L., and R. L. Haney, 1988: Contribution of tropical winds to subseasonal fluctuations in atmospheric angular momentum and length of day. *J. Geophys. Res.*, **93**, 15 973–15 978.

Cadet, D. L., 1983: The monsoon over the Indian Ocean during summer 1975. Part II: Breaks and active monsoons. *Mon. Wea. Rev.*, **111**, 95–108.

——, 1986: Fluctuations of precipitable water over the Indian ocean during the 1979 summer monsoon. *Tellus,* **38A,** 170–177.
——, and S. Greco, 1987: Water vapor transport over the Indian Ocean during the 1979 summer monsoon. *Mon. Wea. Rev.,* **115,** 653–663.
——, and P. Daniel, 1988: Long-range forecast of the break and active summer monsoons. *Tellus,* **40A,** 133–150.
Chang, C-P., 1977: Viscous internal gravity waves and low-frequency oscillations in the tropics. *J. Atmos. Sci.,* **34,** 901–910.
Chen, T-C., 1985: On the time-variation in the tropical energetics of large-scale motions during the FGGE Summer. *Tellus,* **37,** 258–275.
——, 1987: 30–50 day oscillation of 200-mb temperature and 850-mb height during the 1979 northern monsoon. *Mon. Wea. Rev.,* **115,** 1589–1605.
——, and M. Murakami, 1988: The 30–40 day variation of convective activity over the western Pacific Ocean with emphasis on the northwestern region. *Mon. Wea. Rev.,* **116,** 892–906.
——, R. Y. Tzeng, and M. C. Yen, 1988: Development and life-cycle of the Indian monsoon—Effect of the 30–50 day oscillation. *Mon. Wea. Rev.,* **116,** 2183–2199.
Chiswell, S. M., M. Wimbush, and R. Lukas, 1988: Comparison of dynamic height measurements from an inverted echo sounder and an island tide-gauge in the central Pacific. *J. Geophys. Res.,* **93,** 2277–2283.
Dakshinarmuti, J., and R. N. Keshavamurty, 1976: On oscillations of period around one month in the Indian summer monsoon. *Indian J. Meteor. Hydrol. Geophys.* **27,** 201–203.
Dickey, J. O., M. Ghil, and S. L. Marcus, 1991: Extratropical aspects of the 40–50 day oscillation in length-of-day and atmospheric angular momentum. *J. Geophys. Res.,* **96,** 22 643–22 658.
Enfield, D. B., 1987: The intraseasonal oscillation in eastern Pacific sea levels—How is it forced. *J. Phys. Oceanogr.,* **17,** 1860–1876.
——, and R. B. Lukas, 1984: Low-frequency sea level variability along the South American coast in 1982–83. *Trop. Ocean-Atmos. Newslett.,* **28,** 2–4.
Erickson, C. C., M. B. Blumenthal, S. P. Hayes, and P. Ripa, 1983: Wind-generated equatorial Kelvin waves observed across the Pacific Ocean. *J. Phys. Oceanogr.,* **13,** 1622–1640.
Feissel, M., and D. Gambis, 1980: La mise en évidence de variations rapides de la Durée de Jour. C. R. Hebd. *Seances Acad. Sci.,* Ser. B, **291,** 271–273.
Ferranti, L., T. N. Palmer, F. Molteni, and E. Klinker, 1990: Tropical–extratropical interaction associated with the 30–60 day oscillation and its impact on medium and extended range prediction. *J. Atmos. Sci.,* **47,** 2177–2199.
Findlater, J., 1969: A major low-level air current near the Indian Ocean during the northern summer. *Quart. J. Roy. Meteor. Soc.,* **95,** 362–380.
Frostman, T. O., D. W. Martin, and W. Schwerdtfeger, 1967: Annual and semiannual variations in the length of day, related to geophysical effects. *J. Geophys. Res.,* **72,** 5065–5073.
Ghil, M., 1987: Dynamics, statistics and predictability of planetary flow regimes. *Irreversible Phenomena and Dynamical Systems Analysis in Geosciences.* C. Nicolis and G. Nicolis, Eds., D. Reidel, 241–283.
——, and K. Mo, 1991a: Intraseasonal oscillations in the global atmosphere. Part I: Northern Hemisphere and tropics. *J. Atmos. Sci.,* **48,** 752–779.
——, and ——, 1991b: Intraseasonal oscillations in the global atmosphere. Part II: Southern Hemisphere. *J. Atmos. Sci.,* **48,** 780–790.
Gill, A. E., 1980: Some simple solutions for heat-induced tropical circulation. *Quart. J. Roy. Meteor. Soc.,* **106,** 447–463.
Graves, C. E., and J. L. Stanford, 1987: Low-frequency atmospheric oscillations over the southeastern Pacific. *J. Atmos. Sci.,* **44,** 260–264.
Gray, B. M., 1988: Seasonal frequency variations in the 40–50 day oscillation. *J. Climatol.* **8,** 511–519.
Gruber, A., 1974: Wavenumber–frequency spectra of satellite-measured brightness in tropics. *J. Atmos. Sci.,* **31,** 1675–1680.
Gutzler, D. S., and R. A. Madden, 1989: Seasonal variations in the spatial structure of intraseasonal tropical wind fluctuations. *J. Atmos. Sci.,* **46,** 641–660.
——, and ——, 1993: Seasonal variations of the 40–50 day oscillation in atmospheric angular momentum. *J. Atmos. Sci.,* **50,** 850–860.
Hartmann, D. L., and M. L. Michelsen, 1989: Intraseasonal periodicities in Indian rainfall. *J. Atmos. Sci.,* **46,** 2838–2862.
Hendon, H. H., and B. Liebmann, 1990a: A composite study of onset of the Australian summer monsoon. *J. Atmos. Sci.,* **47,** 2227–2240.
——, and ——, 1990b: The intraseasonal (30–50 day) oscillation of the Australian summer monsoon. *J. Atmos. Sci.,* **47,** 2909–2923.
Holland, G. J., 1986: Interannual variability of the Australian summer monsoon at Darwin—1952–82. *Mon. Wea. Rev.,* **114,** 594–604.
Holton, J. R., 1973: On the frequency distribution of atmospheric Kelvin waves. *J. Atmos. Sci.,* **30,** 499–501.
Julian, P. R., and R. A. Madden, 1981: Comments on a paper by T. Yasunari, a quasistationary appearance of 30 to 40 day period in the cloudiness fluctuations during the summer monsoon over India. *J. Meteor. Soc. Japan,* **59,** 435–437.
Kai, K., 1985: Spectrum climatology of the surface winds in Japan. 1: The 40–60 day fluctuations. *J. Meteor. Soc. Japan,* **63,** 873–882.
Kang, I.-S., and K.-M. Lau, 1990: Evolution of tropical circulation anomalies associated with 30–60 day oscillation of globally averaged angular momentum during northern summer. *J. Meteor. Soc. Japan,* **68,** 237–249.
Khalsa, S. J. S., and E. J. Steiner, 1988: A TOVS dataset for study of the tropical atmosphere. *J. Appl. Meteor.,* **27,** 851–862.
Kiladis, G., and K. M. Weickmann, 1992: Circulation anomalies associated with tropical correlation during northern winter. *Mon. Wea. Rev.,* **120,** 1900–1923.
Kindle, J. C., and J. D. Thompson, 1989: The 26-day and 50-day oscillations in the western Indian Ocean—Model results. *J. Geophys. Res.,* **94,** 4721–4736.
Knutson, T. R., and K. M. Weickmann, 1987: 30–60 day atmospheric oscillations: Composite life cycles of convection and circulation anomalies. *Mon. Wea. Rev.,* **115,** 1407–1436.
——, ——, and J. E. Kutzbach, 1986: Global-scale intraseasonal oscillations of outgoing longwave radiation and 250 mb zonal wind during northern hemisphere summer. *Mon. Wea. Rev.,* **114,** 605–623.
Kousky, V. E., 1985: The global climate for December 1984–February 1985—A case of strong intraseasonal oscillations. *Mon. Wea. Rev.,* **113,** 2158–2172.
Krishnamurti, T. N., and P. A. Ardanuy, 1980: The 10 to 20-day westward propagating mode and "breaks in the monsoons." *Tellus,* **32,** 15–26.
——, and D. Subrahmanyam, 1982: The 30–50 day mode at 850 mb during MONEX. *J. Atmos. Sci.,* **39,** 2088–2095.
——, and S. Gadgil, 1985: On the structure of the 30 to 50 day mode over the globe during FGGE, *Tellus,* **37A,** 336–360.
——, D. K. Jayakumar, J. Sheng, N. Surgi, and A. Kumar, 1985: Divergent circulation on the 30 to 50 day time scale. *J. Atmos. Sci.,* **42,** 364–375.
——, D. K. Oosterhof, and A. V. Mehta, 1988: Air–sea interaction on the time scale of 30 to 50 days. *J. Atmos. Sci.,* **45,** 1304–1322.
——, M. Subrahmanyam, D. K. Osterhof, and G. Daughenbaugh, 1990: Predictability of low frequency modes. *Meteor. Atmos. Phys.,* **44,** 63–83.
Kuhnel, I., 1989: Spatial and temporal variation in Australia–Indonesian region cloudiness. *Int. J. Climatol,* **9,** 395–405.

Lambeck, K., and A. Cazenave, 1974: The earth's rotation and atmospheric circulation—ii. The continuum. *Geophys. J. Roy. Astron. Soc.*, **38,** 49–61.

Langley, R. G., R. W. King, I. I. Shapiro, R. D. Rosen, and D. A. Salstein, 1981: Atmospheric angular momentum and the length of day: A common fluctuation with a period near 50 days. *Nature,* **294,** 730–732.

Lau, K.-M., and P. H. Chan, 1983: Short-term climate variability and atmospheric teleconnections from satellite-observed outgoing longwave radiation simultaneous relationships. *J. Atmos. Sci.,* **40,** 2735–2750.

——, and ——, 1985: Aspects of the 40–50 day oscillation during the northern winter as inferred from outgoing longwave radiation. *Mon. Wea. Rev.,* **113,** 1889–1909.

——, and ——, 1986a: Aspects of the 40–50 day oscillation during the northern summer as inferred from outgoing longwave radiation. *Mon. Wea. Rev.,* **114,** 1354–1367.

——, and ——, 1986b: The 40–50 day oscillation and the El Nino/Southern Oscillation—A new perspective. *Bull. Amer. Meteor. Soc.,* **67,** 533–534.

——, G. J. Yang, and S. H. Shen, 1988: Seasonal and intraseasonal climatology of summer monsoon rainfall over East Asia. *Mon. Wea. Rev.,* **116,** 18–37.

——, T. Nakazawa, and C. H. Sui, 1991: Observations of cloud cluster hierarchies over the tropical western Pacific. *J. Geophys. Res.,* **96,** 3197–3208.

Legras, B., and M. Ghil, 1985: Persistent anomalies, blocking and variations in atmospheric predictability. *J. Atmos. Sci.,* **42,** 433–471.

Lindzen, R. S., 1974a: Wave-CISK in the Tropics. *J. Atmos. Sci.,* **31,** 156–179.

——, 1974b: Wave-CISK and tropical spectra. *J. Atmos. Sci.,* **31,** 1447–1449.

Lorenc, A. C., 1984: The evolution of planetary-scale 200-mb divergent flow during the FGGE year. *Quart. J. Roy. Meteor. Soc.,* **110,** 427–441.

Luther, D. S., 1980: Observations of long period waves in the tropical oceans and atmosphere. PhD. thesis, Massachusetts Institute of Technology–Woods Hole Oceanographic Institution, 210 pp.

McBride, J. L., 1983: Satellite-observations of the Southern Hemisphere monsoon during winter MONEX. *Tellus,* **35a,** 189–197.

McPhaden, M. J., 1982: Variability in the central equatorial Indian Ocean: Ocean dynamics. *J. Mar. Res.,* **40,** 157–176.

Madden, R. A., 1986: Seasonal variations of the 40–50 day oscillation in the Tropics. *J. Atmos. Sci.,* **43,** 3138–3158.

——, 1987: Relationships between changes in the length of day and the 40 to 50 day oscillation in the tropics. *J. Geophys. Res.,* **92,** 8391–8399.

——, 1992a: Large intraseasonal variations in wind stress over the tropical Pacific. *J. Geophys. Res.,* **93,** 5333–5340.

——, 1992b: Changes in atmospheric angular momentum associated with the intraseasonal oscillation. *Trends Geophys. Res. Council Sci. Res. Integration Pubs.,* **1,** 263–272.

——, and P. R. Julian, 1971: Description of a 40–50 day oscillation in the zonal wind in the tropical Pacific. *J. Atmos. Sci.,* **28,** 702–708.

——, and ——, 1972a: Description of global-scale circulation cells in the tropics with a 40–50 day period. *J. Atmos. Sci.,* **29,** 1109–1123.

——, and ——, 1972b: Further evidence of global-scale 5-day pressure waves. *J. Atmos. Sci.,* **29,** 1464–1469.

Magaña, V., 1993: The 40- and 50-day oscillations in atmospheric angular momentum at various latitudes. *J. Geophys. Res.,* **98,** 10 441–10 450.

——, and M. Yanai, 1991: Tropical–midlatitude interaction on the time scale of 30 to 60 days during the northern summer of 1979. *J. Climate,* **4,** 180–201.

Markus, S. L., M. Ghil, J. O. Dickey, and T. M. Eubanks, 1990: Origin of the 30–60 day oscillation in the length of day and atmospheric angular momentum: New findings from the UCLA general circulation model. *The Earth's Rotation and Reference Frames for Geodesy and Geodynamics,* G. A. Wilkins, Ed., Springer-Verlag.

Maruyama, T., 1967: Large-scale disturbances in the equatorial lower stratosphere. *J. Meteor. Soc. Japan,* **45,** 391–408.

——, 1968: Time sequence of power spectra of disturbances in the equatorial lower stratosphere in relation to the quasi-biennial oscillation. *J. Meteor. Soc. Japan,* **46,** 327–342.

Matsuo, T., 1984: About 30-day, 40-day, and 50-day period oscillations emerging from time variations of meteorological elements around Japan. *Pap. Meteor. Geophys.,* **35,** 181–197.

Mehta, A. V., and T. N. Krishnamurti, 1988: Interannual variability of the 30–50 day wave motions. *J. Meteor. Soc. Japan,* **66,** 535–548.

Mehta, V. M., and J. E. Ahlquist, 1986: Interannual variability of the 30–50 day activity in the Indian-summer monsoon. *Meteor. Atmos. Phys.,* **35,** 166–176.

Mertz, G. J., and L. A. Mysak, 1984: Evidence for a 40–60 day oscillation over the western Indian ocean during 1976 and 1979. *Mon. Wea. Rev.,* **112,** 383–386.

Mitchum, G. T., and R. Lukas, 1987: The latitude frequency structure of Pacific sea-level variance. *J. Phys. Oceanogr.,* **17,** 2362–2365.

Munk, W. H., and R. L. Miller, 1950: Variation in the earth's angular velocity resulting from fluctuations in atmospheric and oceanic circulation. *Tellus,* **2,** 93–101.

Murakami, M., 1984: Analysis of the deep convective activity over the western Pacific and Southeast Asia 2. Seasonal and intraseasonal variations during northern summer. *J. Meteor. Soc. Japan,* **62,** 88–108.

Murakami, T., 1976: Cloudiness fluctuations during the summer monsoon. *J. Meteor. Soc. Japan,* **54,** 175–181.

——, 1987: Intraseasonal atmospheric teleconnection patterns during the northern hemisphere summer. *Mon. Wea. Rev.,* **115,** 2133–2154.

——, T. Nakazawa, and J. He, 1984: On the 40–50 day oscillations during the 1979 Northern Hemisphere summer: 1: Phase propagation. *J. Meteor. Soc. Japan,* **62,** 440–468.

Mysak, L. A., and G. J. Mertz, 1984: A 40-day to 60-day oscillation in the source region of the Somali Current during 1976. *J. Geophys. Res.,* **89,** 711–715.

Nakazawa, T., 1986: Intraseasonal variations in OLR in the tropics during the FGGE year. *J. Meteor. Soc. Japan,* **64,** 17–34.

——, 1988: Tropical super clusters within intraseasonal variations over the western Pacific. *J. Meteor. Soc. Japan,* **66,** 823–839.

Newton, C. W., 1971: Global angular momentum balance: Earth torques and atmospheric fluxes. *J. Atmos. Sci.,* **28,** 1329–1341.

Nishi, N., 1989: Observational study on the 30–60 day variations in geopotential and temperature fields in the equatorial region. *J. Meteor. Soc. Japan,* **67,** 187–203.

Nogues-Paegle, J., and K. Mo, 1987: Spring-to-summer transitions of global circulations during May–July 1979. *Mon. Wea. Rev.,* **115,** 2088–2102.

Parker, D. E., 1973: Equatorial Kelvin waves at 100 millibars. *Quart. J. Roy. Meteor. Soc.,* **99,** 116–129.

Picaut, J., and J.-M. Verstraete, 1976: Discovery of a 40–50 day-frequency current affecting coasts of Gulf of Guinea. *Cah. ORSTOM Ocean.,* **14,** 3–14.

Quadfasel, D. R., and J. C. Swallow, 1986: Evidence for 50-day period planetary-waves in the south equatorial current of the Indian Ocean. *Deep Sea Res.,* **33,** 1307–1312.

Raghavan, K., D. R. Sikka, and S. V. Gujar, 1975: The influence of cross-equatorial flow over Kenya on the rainfall of western India. *Quart. J. Roy. Meteor. Soc.,* **101,** 1003–1004.

Rosen, R. D., 1993: The axial momentum balance of earth and its fluid envelope. *Surv. Geophys.,* **14,** in press.

——, and D. A. Salstein, 1983: Variations in atmospheric angular-momentum on global and regional scales and the length of day. *J. Geophys. Res.,* **88,** 5451–5470.

Schott, F., M. Fieux, J. Kindle, J. Swallow, and R. Zantopp, 1988: The boundary currents east and north of Madagascar. 2: Direct measurements and model comparisons. *J. Geophys. Res.*, **93,** 4963–4974.

Shetye, S. R., S. C. Shenoi, and D. Sundar, 1991: Observed low-frequency currents in the deep mid-Arabian Sea. *Deep Sea Res.*, **38,** 57–65.

Sikka, D. R., and S. Gadgil, 1980: On the maximum cloud zone and the ITCZ over Indian longitudes during the southwest monsoon. *Mon. Wea. Rev.*, **108,** 1840–1853.

Simmons, A. J., J. M. Wallace, and G. W. Branstator, 1983: Barotropic wave propagation and instability and atmospheric teleconnection patterns. *J. Atmos. Sci.*, **40,** 1363–1392.

Sui, C.-H., and K.-M. Lau, 1992: Multiscale phenomena in the tropical atmosphere over the western Pacific. *Mon. Wea. Rev.*, **120,** 407–430.

von Storch, and J. Xu, 1990: Principal oscillation pattern analysis of the 30- to 60-day oscillation in the tropical troposphere. *Climate Dyn.*, **4,** 175–190.

Wahr, J. M., and A. H. Oort, 1984: Friction and mountain torques and atmospheric fluxes. *J. Atmos. Sci.*, **41,** 190–204.

Wallace, J. M., and C.-P. Chang, 1969: Spectrum analysis of large-scale wave disturbances in the tropical lower troposphere. *J. Atmos. Sci.*, **26,** 1010–1025.

——, and V. E. Kousky, 1968: Observational evidence of Kelvin waves in the tropical stratosphere. *J. Atmos. Sci.*, **25,** 900–907.

Wang, B., and H. Rui, 1990: Synoptic climatology of transient tropical intraseasonal convection anomalies. *Meteor. Atmos. Phys.*, **44,** 43–61.

Weickmann, K. M., 1983: Intraseasonal circulation and outgoing longwave radiation modes during Northern Hemisphere winter. *Mon. Wea. Rev.*, **111,** 1838–1858.

——, and S. J. S. Khalsa, 1990: The shift of convection from the Indian Ocean to the western Pacific Ocean during a 30–60 day oscillation. *Mon. Wea. Rev.*, **118,** 964–978.

——, and P. D. Sardeshmukh, 1994: The atmospheric angular momentum cycle associated with the Madden–Julian oscillation. *J. Atmos. Sci.*, in press.

——, G. R. Lussky, and J. E. Kutzbach, 1985: Intraseasonal (30–60 day) fluctuations of outgoing longwave radiation and 250 mb stream function during northern winter. *Mon. Wea. Rev.*, **113,** 941–961.

——, S. J. S. Khalsa, and J. Eischeid, 1992: The atmospheric angular momentum cycle during the tropical Madden–Julian oscillation. *Mon. Wea. Rev.*, **120,** 2252–2263.

Woodberry, K. E., M. E. Luther, and J. J. O'Brien, 1989: The wind-driven seasonal circulation in the southern tropical Indian Ocean. *J. Geophys. Res.*, **94,** 17 985–18 002.

Wylie, D. P., and B. B. Hinton, 1982: The wind stress patterns over the Indian Ocean during the summer monsoon of 1979. *J. Phys. Oceanogr.*, **12,** 186–199.

Yamagata, T., and Y. Hayashi, 1984: A simple diagnostic model for the 30–50 day oscillation in the tropics. *J. Meteor. Soc. Japan,* **62,** 709–717.

Yanai, M., and T. Maruyama, 1966: Stratospheric wave disturbances propagating over the equatorial Pacific. *J. Meteor. Soc. Japan,* **44,** 291–294.

——, ——, T. Nitta, and Y. Hayashi, 1968: Power spectra of large-scale disturbances over the tropical Pacific. *J. Meteor. Soc. Japan,* **46,** 308–323.

Yasunari, T., 1979: Cloudiness fluctuations associated with the Northern Hemisphere summer monsoon. *J. Meteor. Soc. Japan,* **57,** 227–242.

——, 1980: A quasi-stationary appearance of the 30–40 day period in the cloudiness fluctuations during the summer monsoon over India. *J. Meteor. Soc. Japan,* **58,** 225–229.

——, 1981: Structure of an Indian summer monsoon system with around 40-day period. *J. Meteor. Soc. Japan,* **59,** 336–354.

Zangvil, A., 1975: Temporal and spatial behavior of large-scale disturbances in tropical cloudiness deduced from satellite brightness data. *Mon. Wea. Rev.*, **103,** 904–920.